

T A B L E S

- 3.1 Target parameters
- 3.2 Spectrometer components
- 5.1 Acceptances
- 6.1 Total cross-section data
- 6.2 Diffraction correction
- 6.3 Total cross-section results (unambiguous $K\mu 3$'s)
- 6.4 Total cross-section results (all $K\mu 3$'s)
- 6.5 Regeneration data
- 6.6 Regeneration results
- 6.7 Physical constants
- 8.1 Linear interpolation fits to the data
- 8.2 Regge model fits parameters
- 8.3 Regge model prediction
- 8.4 Nuclear sizes
- 8.5 Sensitivity to changes of input parameters

T A B L E 3.1

Target parameters

	Atomic Number	Length (cm)	Density (g/cm ³)	χ
C	12.00	99.06 ± .005	1.720 ± .002	1.62
Al	27.96	90.17 ± .005	2.714 ± .002	2.02
Cu	63.54	27.00 ± .005	8.93 ± .01	1.76
S _n	118.69	36.06 ± .005	7.30 ± .01	1.74
S _n *	118.69	15.24 ± .005	7.30 ± .01	0.74
Pb	207.19	26.04 ± .005	11.33 ± .02	1.74

T A B L E . 3.2

Components of spectrometer

Object	Relative long. (cm) position	Transverse Dimensions W x H	Effective radiation length $\times 10^{-3}$
RA	- 3214	8 x 18	-
Upst } Decay pipe	- 3202	15 cm \varnothing	-
Downstr } window	- 2118	90 cm \varnothing	7.96
MF	- 2073	86 x 43	4.69
CH1	- 1205	120 x 60	8.01
C2	- 2235	100 x 70	11.4
CH2	- 194	120 x 60	5.03
CH3	- 121	120 x 60	5.65
MAGNET	0	150 x 66	-
CH4	157	140 x 95	6.07
CH5	1330	140 x 95	5.22
C3, C4	1398	122 x 122	29.5
SC	1501	110 x 110	-
μ -filter	1636	-	-
C5	1971	168 x 152	

TABLE 5.1

Spectrometer acceptance integrated over the decay region.

P (GeV/c)	A(Kπ2,p)	A(Kμ3,p)	A(Ke3,p)
25*	+ 0117 +/≈ ± 0004	+ 0026 +/≈ ± 0002	+ 000022 +/≈ ± 000009
35*	+ 1698 +/≈ ± 0015	+ 0306 +/≈ ± 0007	+ 000353 +/≈ ± 000043
45*	+ 2555 +/≈ ± 0030	+ 0758 +/≈ ± 0013	+ 000665 +/≈ ± 000070
55*	+ 4075 +/≈ ± 0045	+ 1065 +/≈ ± 0018	+ 000869 +/≈ ± 000095
65*	+ 5290 +/≈ ± 0063	+ 1200 +/≈ ± 0023	+ 000802 +/≈ ± 000109
75*	+ 5640 +/≈ ± 0060	+ 1251 +/≈ ± 0029	+ 000843 +/≈ ± 000135
85*	+ 5622 +/≈ ± 0101	+ 1278 +/≈ ± 0036	+ 000745 +/≈ ± 000155
95*	+ 5738 +/≈ ± 0125	+ 1289 +/≈ ± 0045	+ 000775 +/≈ ± 000194
105*	+ 5145 +/≈ ± 0147	+ 1176 +/≈ ± 0052	+ 001011 +/≈ ± 000280
115*	+ 5066 +/≈ ± 0193	+ 1293 +/≈ ± 0073	+ 000779 +/≈ ± 000318
125*	+ 5164 +/≈ ± 0275	+ 1192 +/≈ ± 0092	+ 000445 +/≈ ± 000315
135*	+ 4216 +/≈ ± 0305	+ 0996 +/≈ ± 0109	+ 000393 +/≈ ± 000393

N.B.: A(Ke3,p) is the probability for a Ke3 decay to be accepted as a Kμ3 decay.

T A B L E 6.1

Total cross-section data

	Accelerator Pulses	Triggers K	Fully reconstructed Events K	After kinematic cuts	After unambiguous cuts
C	984	348	182	95	33
Al	11694	1913	1094	581	204
Cu	7379	2088	1211	589	200
Sn	8231	1828	960	495	175
Sn	2288	519	312	159	56
Pb	8454	1984	1013	509	174

TABLE 6.2

Diffraction correction. (%)

P (GeV/c)	C	Al	Cu	Sn	Sn*	Pb
25.	0.1	0.2	0.3	0.5	0.2	0.8
35.	0.1	0.3	0.6	1.0	0.4	1.6
45.	0.2	0.6	1.0	1.7	0.7	2.7
55.	0.3	0.6	1.0	2.6	1.0	4.0
65.	0.4	1.2	2.1	3.5	1.4	5.7
75.	0.6	1.6	2.9	4.7	1.8	7.5
85.	0.7	2.0	3.7	6.1	2.4	9.7
95.	0.9	2.5	4.6	7.6	3.0	12.1
105.	1.1	3.0	5.6	9.3	3.6	14.8
115.	1.4	3.7	6.7	11.1	4.3	17.7
125.	1.6	4.3	7.9	13.1	5.1	20.9
135.	1.9	5.0	9.2	15.3	6.0	24.4
145.	2.2	5.6	10.7	17.6	6.9	28.2
155.	2.5	6.6	12.2	20.2	7.9	32.2

TABLE 6.3

 K_{μ} total cross-sections on nuclei. Results in mb for the "unambiguous $K\mu 3^+$ " sample.

p (GeV/c)	C	Al	Cu	Sn	Pb
25.	150.5 ± 15.3	370.7 ± 10.5	707.2 ± 22.0	1276.4 ± 42.1	1312.7 ± 135.9
35.	195.2 ± 5.6	373.0 ± 3.8	795.2 ± 8.4	1316.8 ± 15.3	1339.0 ± 48.8
45.	186.6 ± 3.8	372.2 ± 2.8	774.6 ± 6.1	1326.5 ± 11.1	1364.9 ± 35.6
55.	169.3 ± 3.8	375.6 ± 2.8	771.7 ± 6.1	1292.3 ± 10.9	1316.9 ± 35.2
65.	166.1 ± 4.2	371.8 ± 3.1	783.6 ± 7.0	1291.8 ± 12.4	1246.8 ± 40.0
75.	165.6 ± 5.0	369.1 ± 3.7	775.2 ± 8.3	1307.1 ± 14.9	1246.6 ± 47.6
85.	196.1 ± 6.4	378.5 ± 4.7	770.8 ± 10.2	1289.3 ± 18.3	1308.3 ± 60.0
95.	197.5 ± 8.1	367.6 ± 5.9	760.7 ± 12.9	1269.0 ± 23.2	1246.5 ± 73.5
105.	197.0 ± 10.3	374.1 ± 7.6	801.1 ± 16.5	1306.9 ± 29.4	1476.3 ± 98.3
115.	215.4 ± 14.3	368.9 ± 9.9	768.1 ± 20.8	1311.0 ± 37.4	1389.7 ± 122.5
125.	185.6 ± 15.7	364.0 ± 12.1	780.0 ± 27.3	1270.3 ± 47.0	1382.2 ± 163.0
135.	146.5 ± 20.1	361.9 ± 15.6	754.9 ± 33.9	1358.9 ± 64.5	1535.2 ± 205.6
145.	143.6 ± 26.3	360.0 ± 20.5	774.6 ± 43.4	1226.5 ± 77.2	1168.8 ± 263.5
155.	215.1 ± 30.0	442.8 ± 31.4	720.7 ± 57.6	1209.3 ± 98.6	1353.6 ± 344.6
					2109.6 ± 163.4

N.B.: Statistical errors only.

TABLE 6.4

$\bar{\chi}_L$ total cross-sections on nuclei. Results in mb for the "all Ku3" sample.

p (GeV/c)	C	Al	Cu	Sn	Pb
25.	197.7 ± 13.0	363.4 ± 8.8	749.1 ± 16.2	1306.4 ± 34.7	1238.9 ± 108.4
35.	167.7 ± 3.3	371.5 ± 2.5	777.3 ± 4.9	1311.3 ± 9.1	1336.4 ± 29.1
45.	164.9 ± 2.2	371.1 ± 1.6	769.9 ± 3.6	1319.3 ± 6.5	1308.6 ± 20.6
55.	150.6 ± 2.2	371.0 ± 1.6	780.7 ± 3.6	1297.8 ± 6.4	1298.8 ± 20.4
65.	144.7 ± 2.4	372.0 ± 1.8	782.2 ± 4.0	1300.5 ± 7.2	1275.0 ± 23.1
75.	180.0 ± 2.9	372.2 ± 2.2	777.3 ± 4.8	1291.5 ± 8.7	1272.9 ± 28.1
85.	192.7 ± 3.8	371.8 ± 2.0	773.7 ± 6.0	1296.0 ± 11.1	1263.0 ± 35.3
95.	191.5 ± 4.8	372.5 ± 3.0	782.3 ± 7.6	1283.8 ± 14.1	1299.6 ± 45.6
105.	184.0 ± 4.1	372.7 ± 4.7	777.3 ± 10.1	1288.3 ± 18.4	1344.4 ± 59.3
115.	167.1 ± 6.0	380.7 ± 6.3	793.4 ± 13.4	1306.8 ± 24.2	1369.8 ± 79.7
125.	153.5 ± 10.4	369.7 ± 8.0	766.9 ± 17.2	1317.5 ± 32.1	1327.3 ± 101.7
135.	164.4 ± 13.6	345.1 ± 10.1	791.8 ± 23.4	1293.3 ± 41.6	1246.8 ± 136.8
145.	173.2 ± 17.4	394.5 ± 14.8	759.7 ± 29.6	1270.5 ± 54.4	1335.7 ± 175.4
155.	166.0 ± 23.1	464.7 ± 19.3	726.4 ± 39.2	1230.9 ± 71.9	1460.1 ± 249.5
					2004.8 ± 110.5

N.B.: Statistical errors only.

T A B L E 6.5

Regeneration data

	A1	Cu	Sn	Pb	n + -
Pulses	8867	6833	6765	5904	3743
Trigger	1743 K	1776 K	1848 K	1547 K	1110 K
Recon- structed	969 K	929 K	953 K	997 K	511 K
KPI2	60937	40456	34637	24131	18962
KMU3	10389	6456	12800	9848	-

TABLE 6.6

K_S coherent regeneration on nuclei. Results in mb for $\left| \frac{f(0) - \bar{F}(0)}{p} \right|$

p (GeV/c)	Al		Cu		Sn		Pb	
	+	-	+	-	+	-	+	-
25.	3.92	+/- .22	8.10	+/- .55	12.02	+/- .66	16.90	+/- 1.01
35.	3.12	+/- .06	6.25	+/- .15	9.42	+/- .19	13.97	+/- .31
45.	2.64	+/- .04	4.98	+/- .09	8.04	+/- .12	11.95	+/- .19
65.	2.42	+/- .04	4.60	+/- .08	7.23	+/- .10	10.65	+/- .17
85.	2.21	+/- .04	4.00	+/- .08	6.52	+/- .10	9.64	+/- .17
105.	2.01	+/- .04	3.63	+/- .08	6.90	+/- .11	8.69	+/- .18
125.	1.83	+/- .04	3.42	+/- .09	5.32	+/- .12	7.96	+/- .20
95.	1.74	+/- .05	3.31	+/- .12	5.10	+/- .14	7.65	+/- .24
115.	1.67	+/- .05	3.17	+/- .15	4.74	+/- .18	7.11	+/- .30
125.	1.60	+/- .05	3.21	+/- .19	4.83	+/- .23	6.76	+/- .36
135.	1.29	+/- .11	2.36	+/- .16	4.92	+/- .34	6.87	+/- .49
			2.53	+/- .27	6.71	+/- .44	6.35	+/- .52

N.B.: Statistical errors only.

TABLE 6.7

Physical constants.

$$\xi_s = 1/\Gamma_s = (0.8930 \pm 0.0023) \times 10^{-10} \text{ sec}$$

$$\xi_L = 1/\Gamma_L = (518.1 \pm 4) \times 10^{-10} \text{ sec}$$

$$\Delta m = m_L - m_s = (0.5349 \pm .0023) \times 10^{-10} \text{ sec}^{-1}$$

$$\text{BR}(K_s \rightarrow \pi^+ \pi^-) = 0.6827 \pm 0.0025$$

$$\text{BR}(K_L \rightarrow K\mu\nu) = 0.271 \pm 0.005$$

$$|\eta_+| = (2.183 \pm 0.023) \times 10^{-3}$$

$$\text{Arg } \eta_+ = (45 \pm 1.2)^\circ$$

TABLE 8.1

Linear interpolation fits

TOTAL CROSS-SECTIONS (25 + 135 GeV)

	Unambiguous $\kappa\mu_3$		All $\kappa\mu_3$	
	A	B	A	B
C	188 ± 5	+ 0.03 ± .08	188.4 ± 3	0 ± .05
Al	373 ± 4	0.0 ± .06	372 ± 2	0 ± .04
Cu	774 ± 9	.05 ± .13	771 ± 5	+ .11 ± .08
Sn	1320 ± 15	- .26 ± .27	1324 ± 10	- .34 ± .15
Sn*	1328 ± 50	- .23 ± .76	1317 ± 30	- .32 ± .47
Pb	2105 ± 24	- .83 ± .36	2100 ± 15	- .74 ± .21

REGENERATION (25 + 135 GeV)

	γ	α
C	13.77 ± 1.22	0.397 ± .021
Al	24.33 ± 2.04	0.422 ± .020
Cu	59.1 ± 6.0	0.359 ± .025
Sn	82.0 ± 6.8	0.392 ± .020
Pb	126.6 ± 11.5	0.381 ± .022

Note: For C, a fit from 4.5 to 135 GeV gives $\gamma = 13.78 \pm 0.15$,
 $\alpha = 0.397 \pm 0.003$.

TABLE 8.2

Regge fit parameters of kaon-, pion-, and nucleon-nucleon total cross-sections.

Fit		χ^2	a_p	b_p	c_p	γ_0	α_0	γ_p	α_p	a_n	b_n	c_n
(i)	K	-0.1	17.1771	2104	5.9533	7.8657	4.4240	1.6819	0.6271	17.6764	0.0479	22253 7.4216
	π	1.21	52.2018	2dd04	2A.2676	11.8649	4.4240	2.7338	0.0000	17.6764	0.0479	0.0151 7.4216
	P	1.00	38.3964	4349	63.62039	24.7661	4.373	3.0914	0.0000	38.4860	0.0776	3935 41.1164
(ii)	K	-0.1	17.1756	2102	6.0775	7.8641	4.4240	1.6300	0.6270	17.6857	0.0462	2212 7.1652
	π	1.21	22.2611	2d12	24.7918	11.8190	4.4000	2.7338	0.0000	17.6857	0.0462	0.0143 7.1652
	P	1.02	48.3656	4304	63.6481	26.3519	4.201	2.7462	0.0000	38.4986	0.0765	39.1518
(iii)	K	-0.1	17.1971	1941	5.9691	8.0176	3.970	1.6449	0.6270	17.7396	0.0444	3758 4.2104
	π	1.21	22.0231	2976	31.7013	16.7763	3.970	2.7338	0.0000	17.7396	0.0444	0.0137 4.2104
	P	1.05	38.3776	4275	62.4541	28.0647	3.970	2.7338	0.0000	38.5160	0.0756	3620 37.8723
(iv)	K	1.01	17.1954	1943	5.1502	8.0676	3.920	1.6200	0.6299	17.7413	0.0446	39317 6.9317
	π	1.21	22.0231	2976	31.6015	10.7663	3.970	2.7338	0.0000	17.7413	0.0446	0.0141 6.9317
	P	1.05	38.3749	4280	62.7250	28.5246	3.970	4.916	0.0000	38.5150	0.0756	3605 37.5618
			0.0161	1.3512	3.5524	0.0000	4.994	6.956	0.0000	38.5150	0.0756	3605 37.5618

N.B.: From a separate fit to the $\pi^+ - \pi^-$ difference, we get $\gamma_{\pi^2} = 73^{+0.06}$ and $\alpha_p = 0.57^{+0.01}$.

TABLE 8.3

Results and predictions from the Regge parametrization of the kaon-nucleon amplitudes.

P (GeV/c)	$K^+ p$	$K^- p$	$K^+ n$	$K^- n$	$\bar{K} n$	$\bar{K} p$	$K^+ \pi^0 n$	$K^+ \pi^0 p$	$K_L p \bar{K}_S p$
	σ_T (mb)	a	σ_T (mb)	a	σ_T (mb)	a	$d\sigma/dt$	$ F-E /p$	ϕ
5.	17.164	+0.417	24.031	+0.93	17.712	+1.29	22.201	+0.80	+0.21
15.	17.350	+0.104	21.612	+0.56	17.748	+0.59	20.108	+0.41	+1.16
25.	17.619	+0.107	20.549	+0.59	18.009	+0.23	19.712	+0.46	+1.22
35.	17.850	+0.072	20.551	+0.04	19.216	+0.02	19.606	+0.52	+0.74
45.	18.054	+0.046	20.418	+0.08	18.408	+0.14	19.599	+0.58	+0.87
55.	18.237	+0.030	20.361	+0.72	18.580	+0.26	19.633	+0.63	+0.90
65.	18.402	+0.17	20.346	+0.75	18.737	+0.33	19.688	+0.67	+0.93
75.	18.553	+0.006	20.356	+0.78	18.882	+0.40	19.752	+0.70	+0.95
85.	18.643	+0.02	20.379	+0.81	19.016	+0.46	19.821	+0.73	+0.98
95.	18.622	+0.10	20.412	+0.83	19.141	+0.51	19.893	+0.75	+0.99
105.	18.943	+0.10	20.451	+0.84	19.258	+0.55	19.965	+0.77	+0.99
115.	19.057	+0.21	20.494	+0.86	19.369	+0.58	20.037	+0.79	+0.99
125.	19.164	+0.26	20.539	+0.87	19.473	+0.61	20.108	+0.81	+0.99
135.	19.266	+0.30	20.656	+0.88	19.572	+0.64	20.177	+0.82	+0.99
145.	19.343	+0.33	20.694	+0.89	19.667	+0.66	20.245	+0.83	+0.99
155.	19.455	+0.36	20.642	+0.90	19.757	+0.68	20.312	+0.84	+0.99
165.	19.543	+0.39	20.731	+0.91	19.844	+0.70	20.377	+0.85	+0.99
175.	19.628	+0.41	20.774	+0.92	19.927	+0.71	20.441	+0.86	+0.99

TABLE 8.4

Nuclear size parameters (Fermis)

	A	Z	R	S	$\sqrt{\langle r^2 \rangle}$
D	2	1	-	-	2.095
Be	9	4	-	-	2.519
C	12	6	-	-	2.470
Al	27	13	3.070	.519	3.060
Fe	56	26	3.980	.569	3.737
Cu	64	29	4.205	.569	3.882
Cd	112	48	5.382	.533	4.615
Sn	119	50	5.320	.576	4.643
W	184	74	6.520	.491	5.370
Pb	207	82	6.670	.503	5.494
U	238	92	6.962	.605	5.843

TABLE 8.5.1

Sensitivity of the calculated cross-sections and regenerations to changes in input parameters at 10 GeV/c.

	$\Delta R_p =$ +0.1 fm	$\Delta R_p =$ +0.1 fm	$\Delta R_n =$ +0.1 fm	$\Delta \beta =$ +1 GeV ²	$\Delta \delta =$ +1 mb	$\Delta \sigma(K^0 p)$ +1 mb	$\Delta \sigma(\bar{K}^0 n)$ +1 mb	$\Delta \sigma(\bar{K}^0 p)$ +1 mb	$\Delta \sigma(\bar{K}^0 n)$ +1 mb
$\Delta \sigma_T$	C Al Cu (%) Sn Pb	• 40 • 56 • 50 • 55 • 53	• 71 • 0.3 1.16 1.22 1.26	• 31 • 4.9 • 5.9 • 6.7 • 7.4	• 2.6 • 0.1 • 2.4 • 2.1 • 1.9	• 0.1 • 99 • 83 • 7.0 • 5.8	• 1.1 • 0.6 • 0.1 • 9.6 • 4.0	• 1.1 • 0.6 • 0.1 • 9.6 • 4.0	• 0.3 • 9.6 • 5.6 • 8.1 • 7.2
	C Al Cu (%) Sn Pb	• 50 • 67 • 65 • 67 • 60	1.25 1.07 2.15 2.32 2.51	• 7.0 1.22 1.52 1.77 2.01	• 2.9 • 3.4 • 3.0 • 3.7 • 4.1	• 0.5 • 9.1 • 0.7 • 1.4 • 9.1	• 7.0 • 7.40 • 7.07 • 8.37 • 8.66	• 7.0 • 7.40 • 7.07 • 8.37 • 8.66	• 6.66 • 6.56 • 6.46 • 6.40 • 6.25
	C Al Cu (%) Sn Pb	• 50 • 67 • 65 • 67 • 60	1.25 1.07 2.15 2.32 2.51	• 7.0 1.22 1.52 1.77 2.01	• 2.9 • 3.4 • 3.0 • 3.7 • 4.1	• 0.5 • 9.1 • 0.7 • 1.4 • 9.1	• 7.0 • 7.40 • 7.07 • 8.37 • 8.66	• 7.0 • 7.40 • 7.07 • 8.37 • 8.66	• 6.66 • 6.56 • 6.46 • 6.40 • 6.25
	C Al Cu (%) Sn Pb	• 50 • 67 • 65 • 67 • 60	1.25 1.07 2.15 2.32 2.51	• 7.0 1.22 1.52 1.77 2.01	• 2.9 • 3.4 • 3.0 • 3.7 • 4.1	• 0.5 • 9.1 • 0.7 • 1.4 • 9.1	• 7.0 • 7.40 • 7.07 • 8.37 • 8.66	• 7.0 • 7.40 • 7.07 • 8.37 • 8.66	• 6.66 • 6.56 • 6.46 • 6.40 • 6.25
	C Al Cu (%) Sn Pb	• 50 • 67 • 65 • 67 • 60	1.25 1.07 2.15 2.32 2.51	• 7.0 1.22 1.52 1.77 2.01	• 2.9 • 3.4 • 3.0 • 3.7 • 4.1	• 0.5 • 9.1 • 0.7 • 1.4 • 9.1	• 7.0 • 7.40 • 7.07 • 8.37 • 8.66	• 7.0 • 7.40 • 7.07 • 8.37 • 8.66	• 6.66 • 6.56 • 6.46 • 6.40 • 6.25
	C Al Cu (%) Sn Pb	• 50 • 67 • 65 • 67 • 60	1.25 1.07 2.15 2.32 2.51	• 7.0 1.22 1.52 1.77 2.01	• 2.9 • 3.4 • 3.0 • 3.7 • 4.1	• 0.5 • 9.1 • 0.7 • 1.4 • 9.1	• 7.0 • 7.40 • 7.07 • 8.37 • 8.66	• 7.0 • 7.40 • 7.07 • 8.37 • 8.66	• 6.66 • 6.56 • 6.46 • 6.40 • 6.25

TABLE 8.5.2

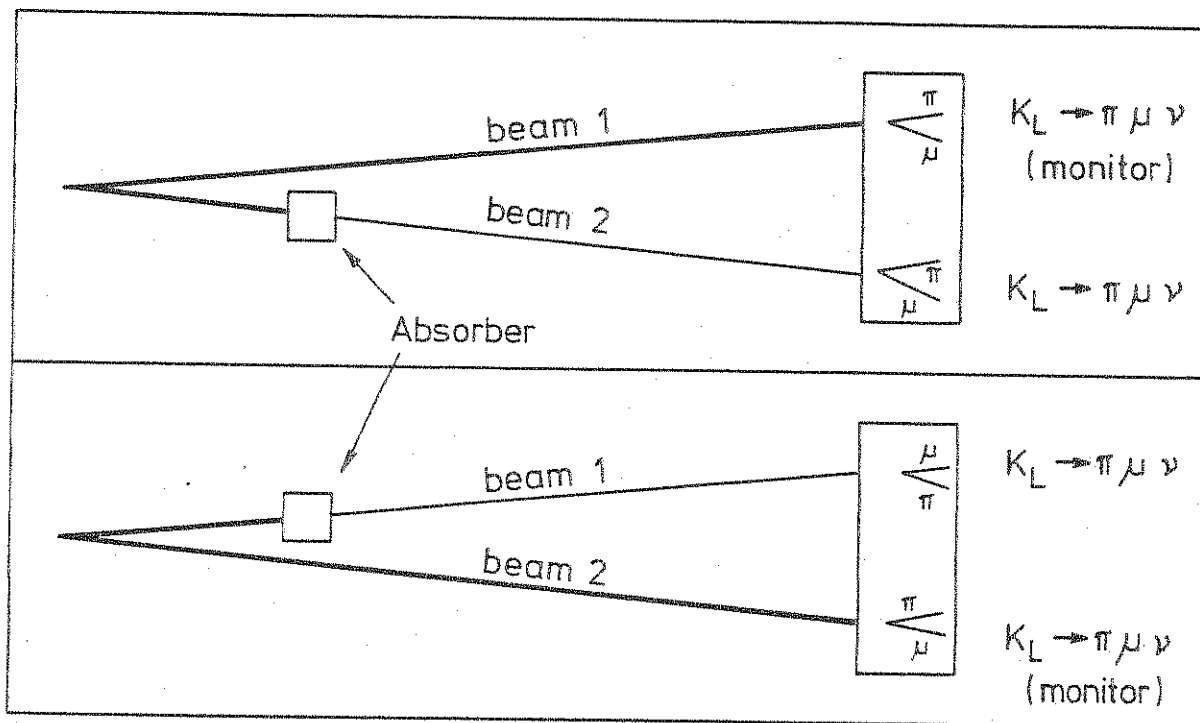
Sensitivity of the calculated cross-sections and regenerations to changes in input parameters at 100 GeV/c.

		$\Delta R_p =$ +0.1 fm	$\Delta R_p =$ +0.1 fm	$\Delta R_p =$ +0.1 fm	$\Delta \beta =$ +1 GeV ²	$\Delta \delta =$ +1 GeV ⁴	$\Delta \sigma(\bar{K}^0 p)$ +1 mb	$\Delta \sigma(\bar{K}^0 n)$ +1 mb	$\Delta \sigma(\bar{K}^0 p)$ +1 mb	$\Delta \sigma(\bar{K}^0 n)$ +1 mb
		C	* 50	* 77	* 27	* 28	* 0.1	1.10	1.10	1.08
		Al	* 68	1.09	* 42	* 25	* 0.6	1.07	* 57	1.04
		Cu	* 69	1.20	* 51	* 25	* 0.0	1.04	* 53	1.01
(%)		Sn	* 64	1.22	* 55	* 22	* 0.0	1.03	* 72	1.01
		Pb	* 60	1.22	* 63	* 21	* 0.0	* 99	* 62	1.01
	$\Delta \sigma_T$	C	* 36	1.08	* 73	* 1.36	* 0.1	* 26.36	* 26.30	32.44
		Al	* 41	1.56	1.16	* 1.09	* 0.1	* 24.40	* 25.78	29.62
		Cu	* 26	1.69	1.44	* 0.65	* 0.1	* 21.93	* 25.29	32.06
(%)		Sn	* 11	1.76	1.66	* 32	* 0.0	* 19.60	* 25.07	31.73
		Pb	* 10	1.85	1.67	* 0.8	* 0.1	* 18.04	* 24.97	31.61
	$\Delta \frac{\bar{E}-\bar{E}}{P}$	C	* 36	1.08	* 73	* 1.36	* 0.1	* 26.36	* 26.30	32.44
		Al	* 41	1.56	1.16	* 1.09	* 0.1	* 24.40	* 25.78	29.62
		Cu	* 26	1.69	1.44	* 0.65	* 0.1	* 21.93	* 25.29	32.06
(%)		Sn	* 11	1.76	1.66	* 32	* 0.0	* 19.60	* 25.07	31.61
		Pb	* 10	1.85	1.67	* 0.8	* 0.1	* 18.04	* 24.97	31.61

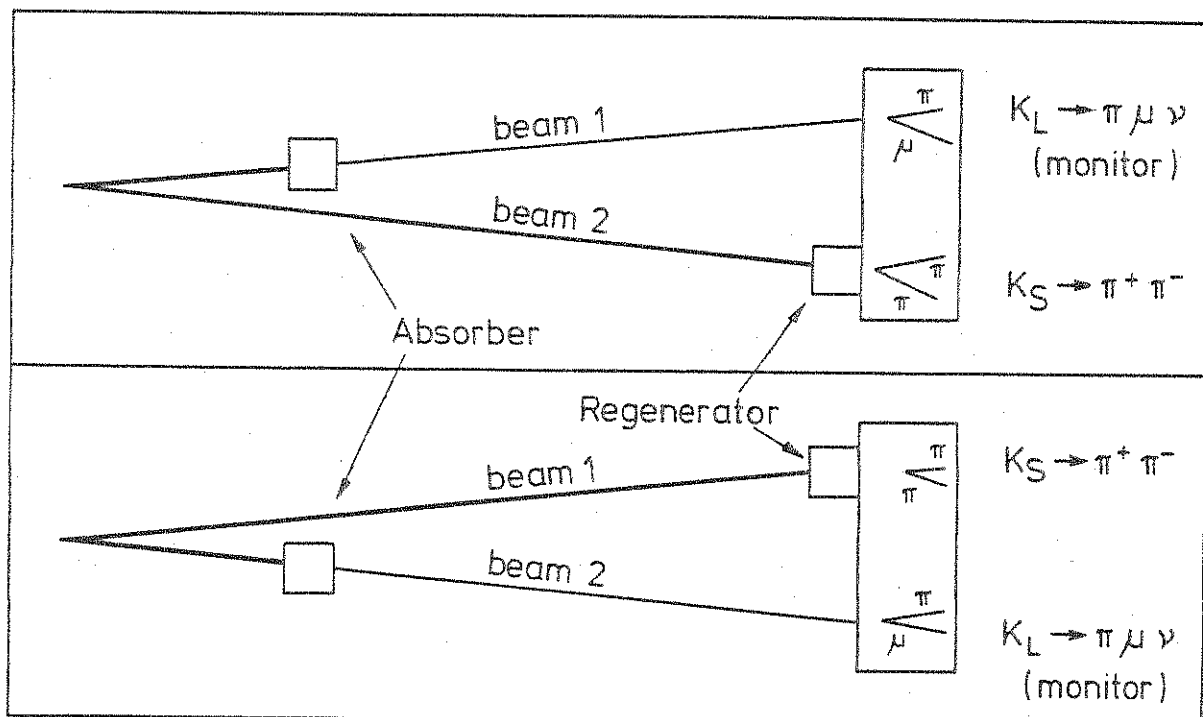
FIGURES

Fig. 2.1 Principle of K_L total cross-section measurement method.

Fig. 2.2 Principle of K_S regeneration measurement method.



K_L Total Cross-section Measurement.



K_S Regeneration Measurement

Fig. 3.1 M4 Beam line. Shown are the main components of the neutral double-beam and their relative positions.

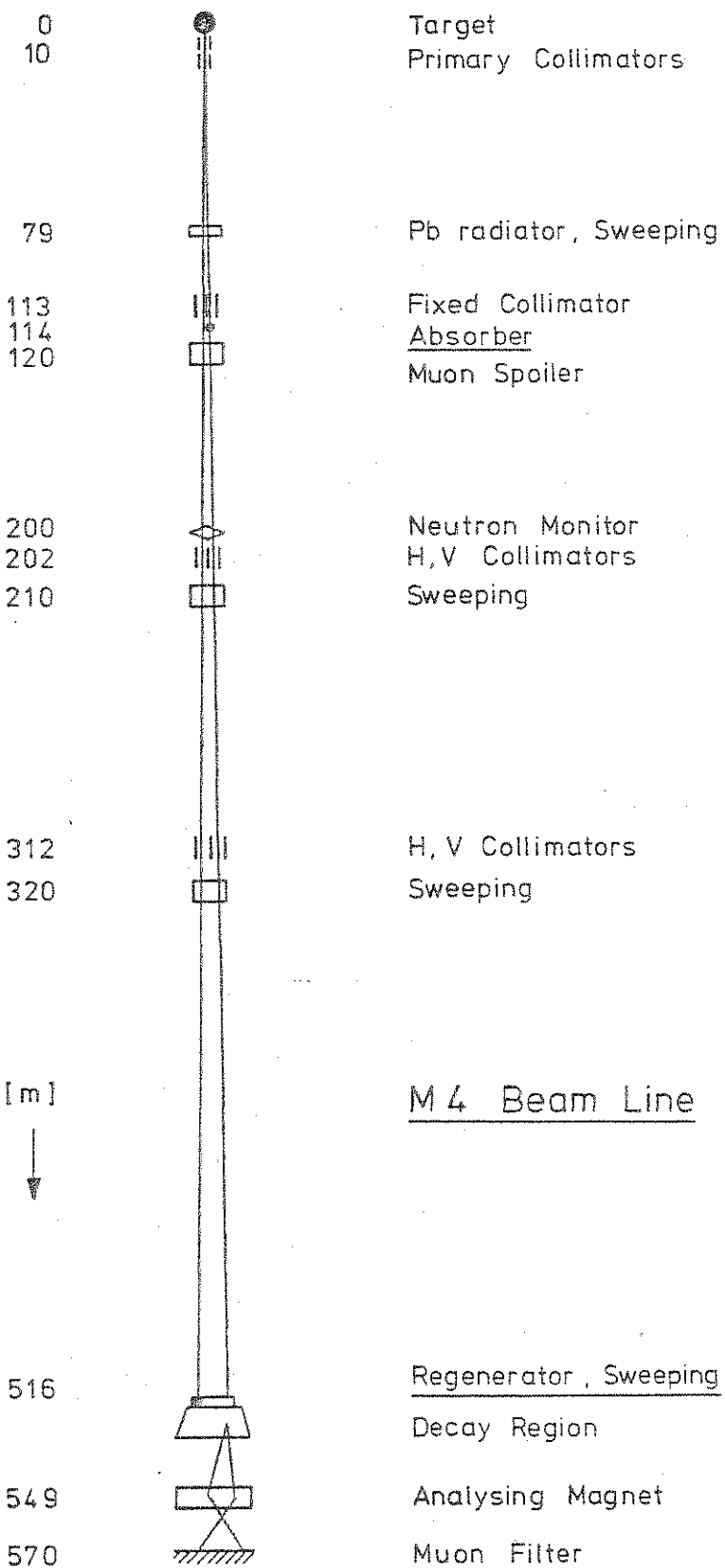


Fig. 3.2 The detection apparatus. C1 and MF are defining the decay region. C2-C5 are the counter hodoscopes. Ch1 to Ch5 are the multiwire proportional chambers. The analysing magnet is between Ch3 and Ch4.

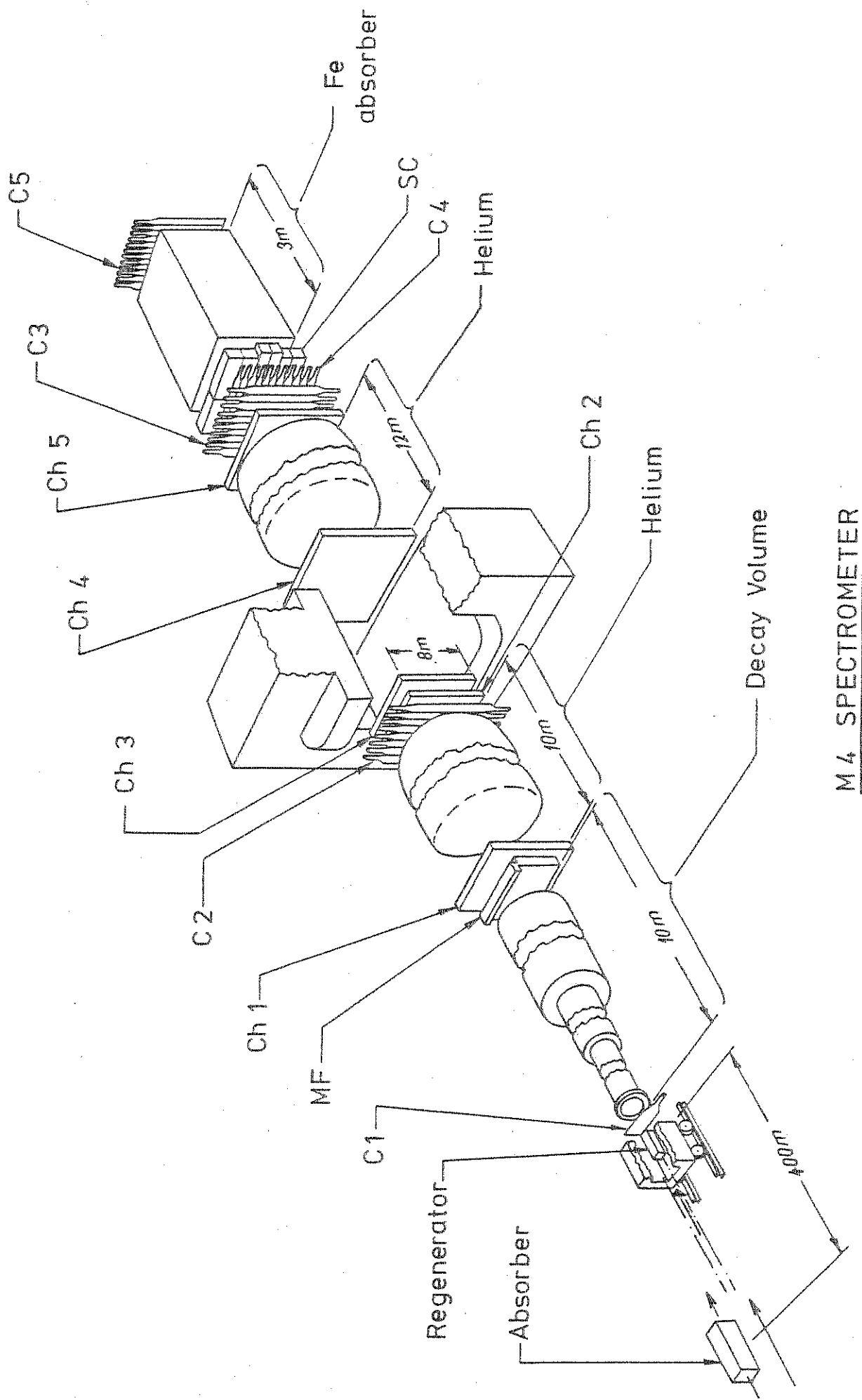


Fig. 3.3 M4 K_L spectrum.

The K_L spectrum is calculated from observed $K\mu 3$ decays in the apparatus.

$K_L / \text{GeV}/c / \text{Str. Inc. Proton}$

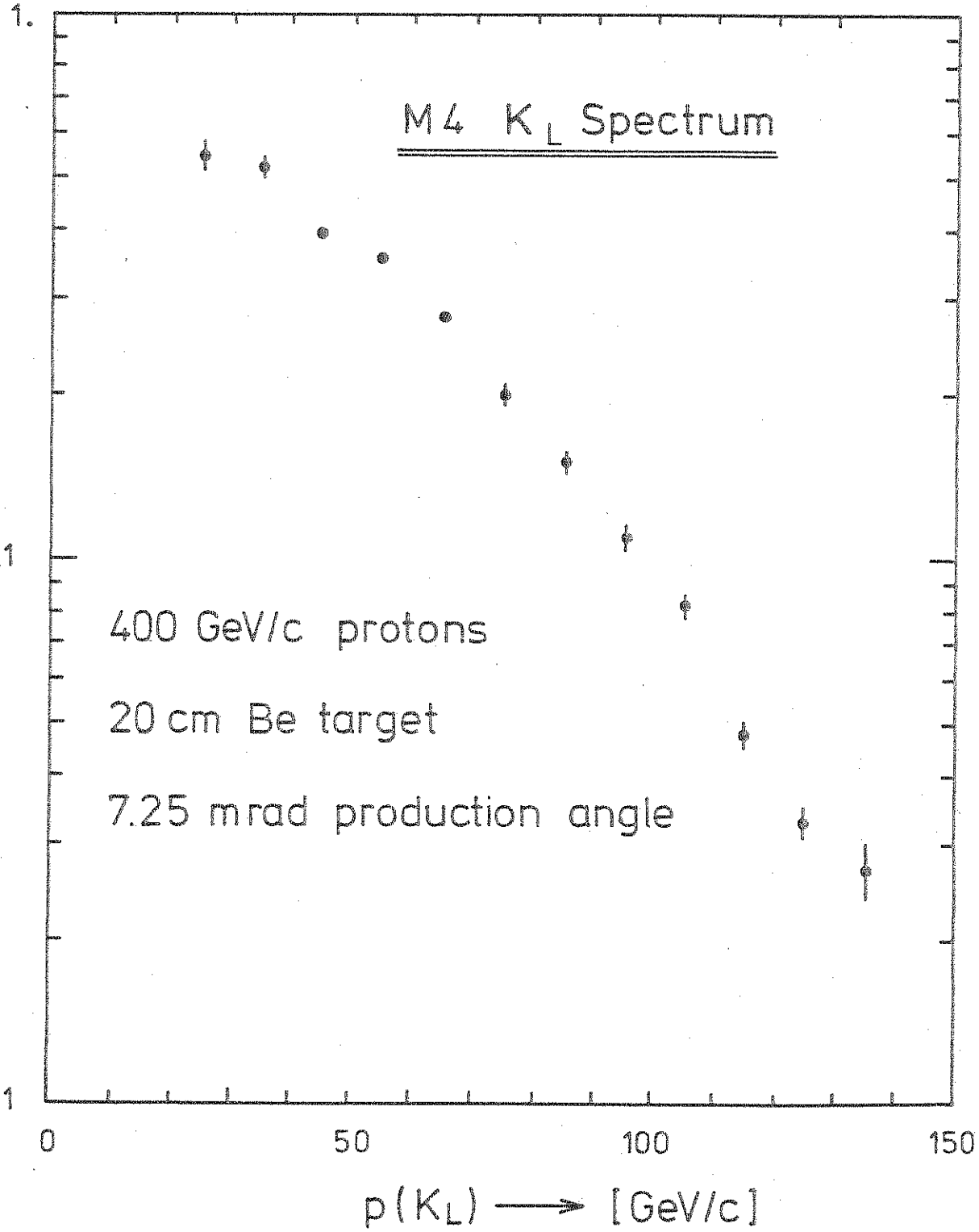


Fig. 3.4 Absorber block moving machine. The absorbers were mounted on a rotating frame.

Fig. 3.5 Regenerator block moving machine. A right angle shaft and four cams were used to translate the regenerator vertically.

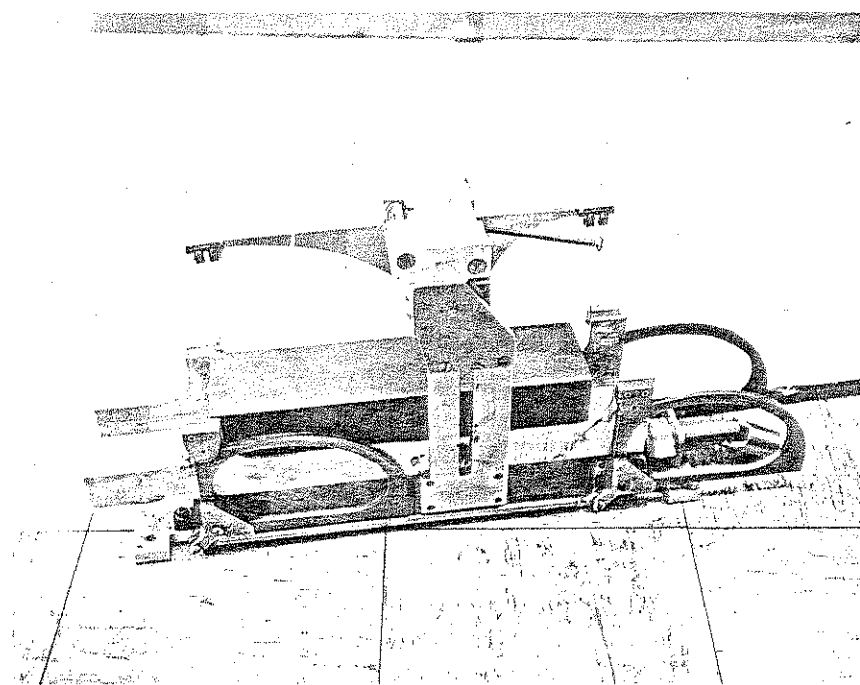
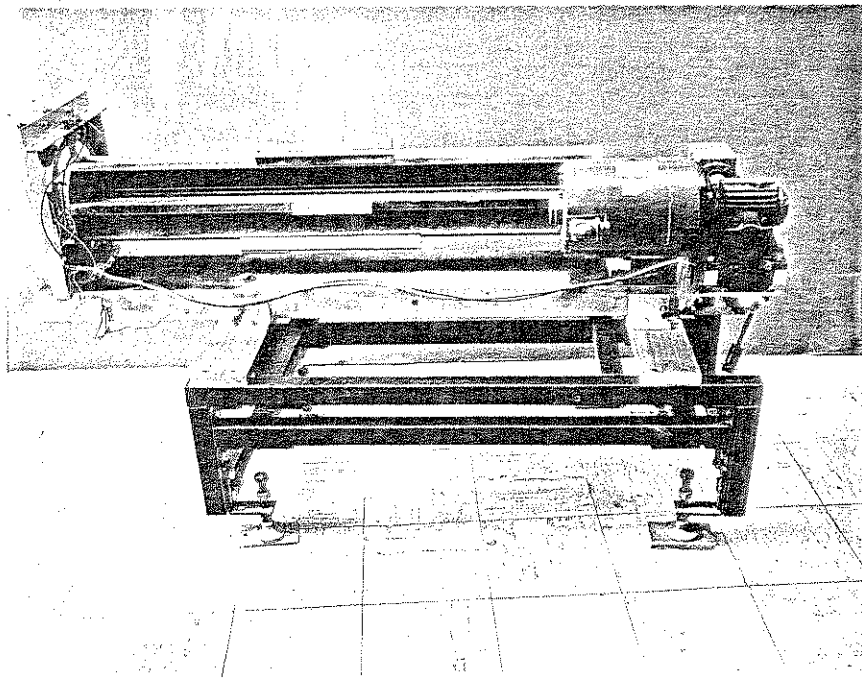


Fig. 4.1 Electronics. From left to right: the trigger counters, the first level logic, the second level logic (C2X), the camac. The EVENT, RESET and VETO signals are the main control signals interacting with the computer.

ELECTRONICS

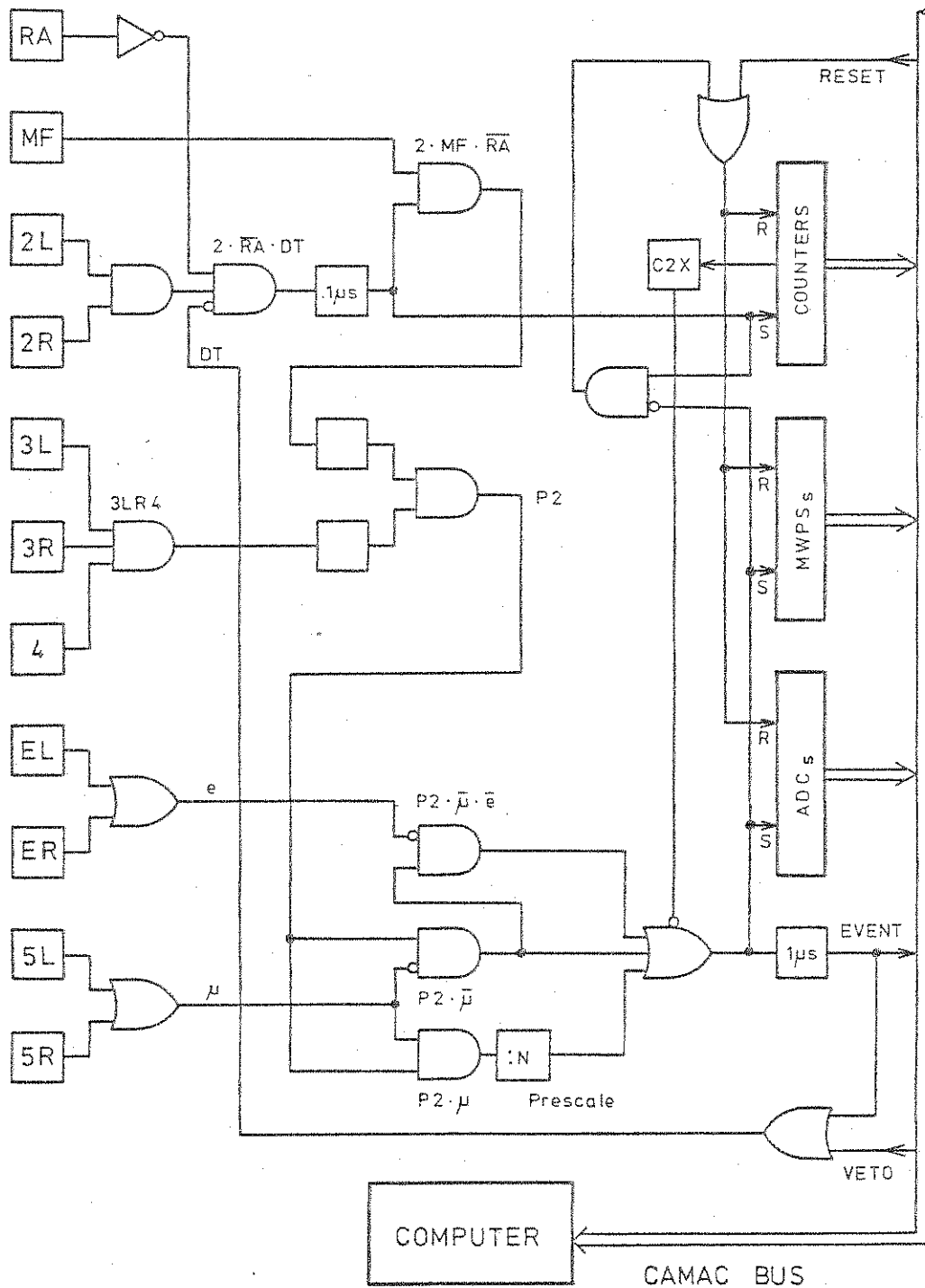


Fig. 5.1 Deviation² vs. 1/p².

Data: —

M.C.: e

[GeV/c]

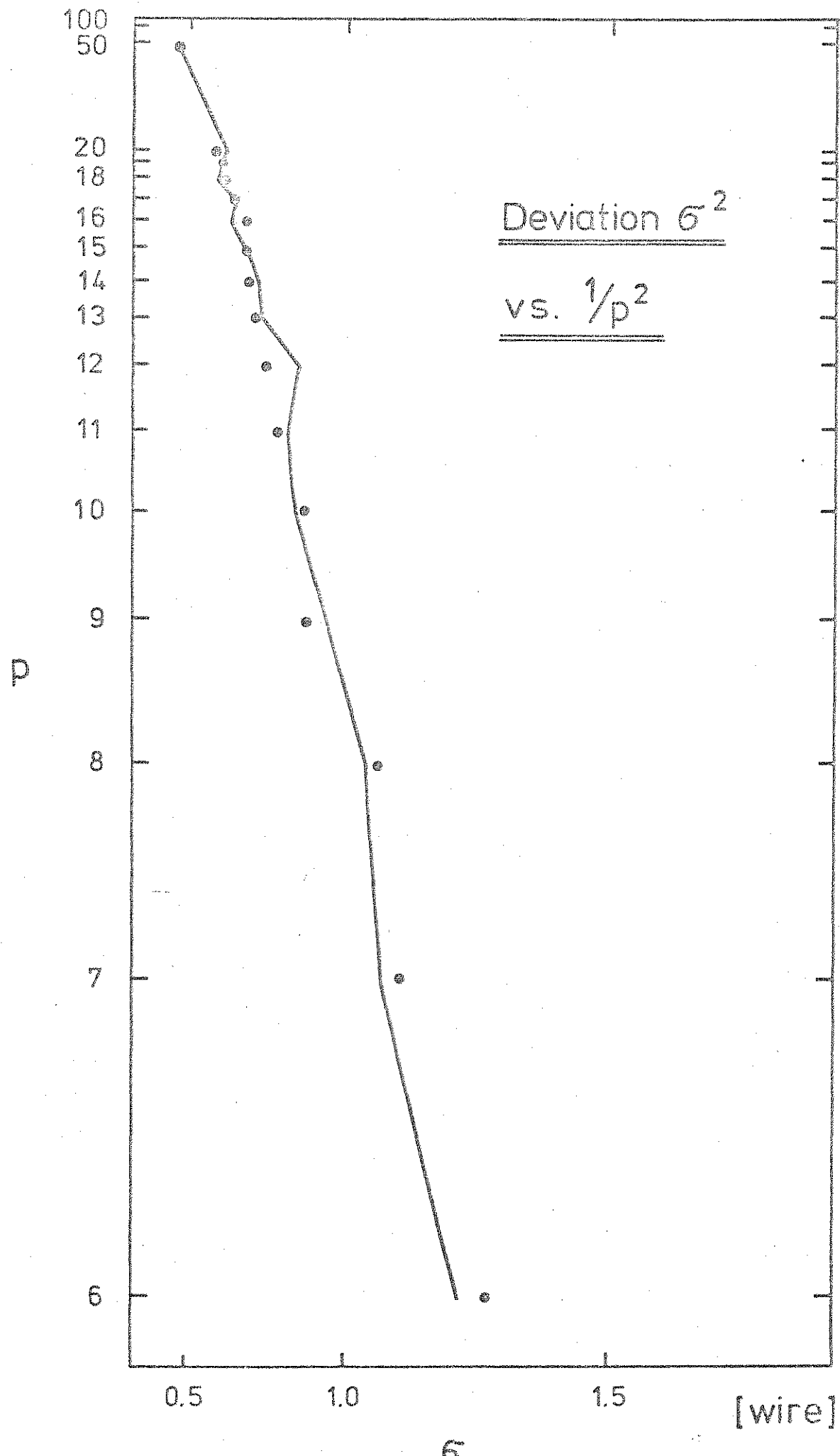
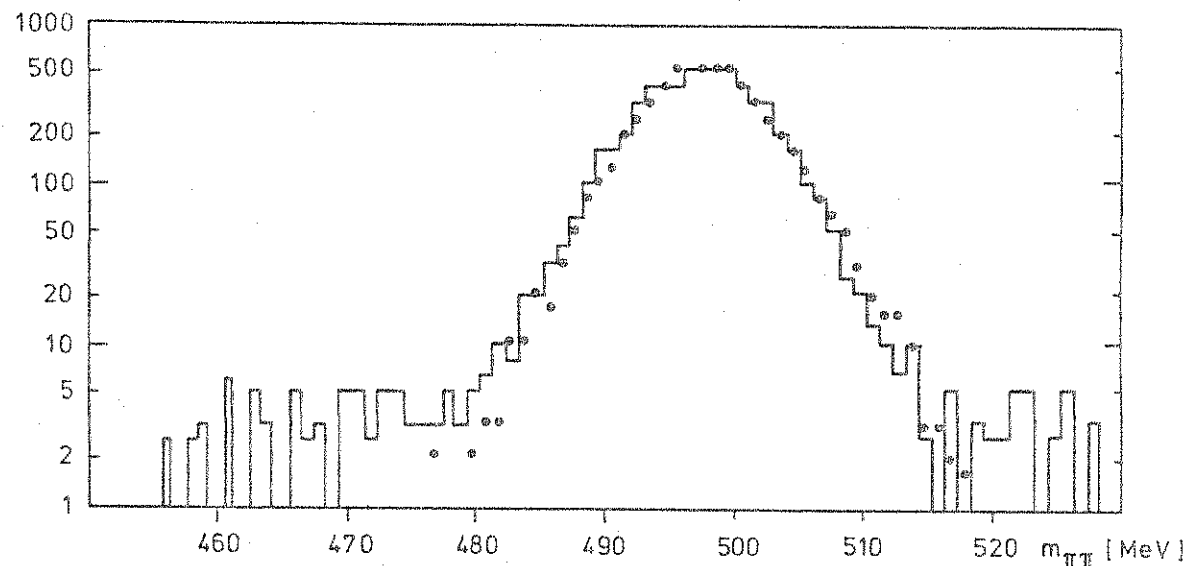
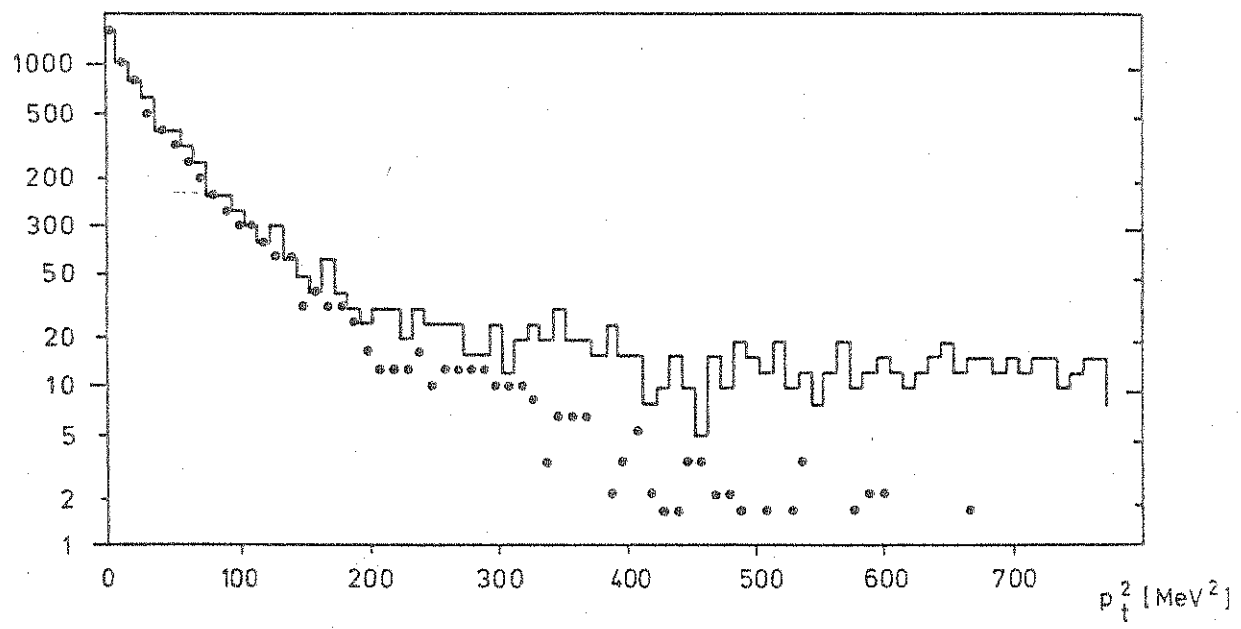


Fig. 5.2 K_S invariant mass $m_{\pi\pi}$.
50 GeV/c $\leq p \leq$ 60 GeV/c ,
 $0 \leq p_t^2 \leq 150 (\text{MeV}/c)^2$.
Data: _____
M.C.: @

Fig. 5.3 K_S transferred momentum squared p_t^2 .
50 GeV/c $\leq p \leq$ 60 GeV/c ,
 $487 \text{ MeV} \leq m_{\pi\pi} \leq 507 \text{ MeV}$.
Data: _____
M.C.: @



K_s In variant mass



K_s transverse momentum squared

Fig. 5.4 K_S invariant mass resolution as a function of kaon momentum.
 $0 < p_t^2 < 150 \text{ (MeV/c)}^2$.
Data: 
M.C.: 

Fig. 5.5 K_S transferred momentum squared resolution as a function of kaon momentum.
 $477 \text{ MeV} < m_{\pi\pi} < 517 \text{ MeV}$.
Data: 
M.C.: 

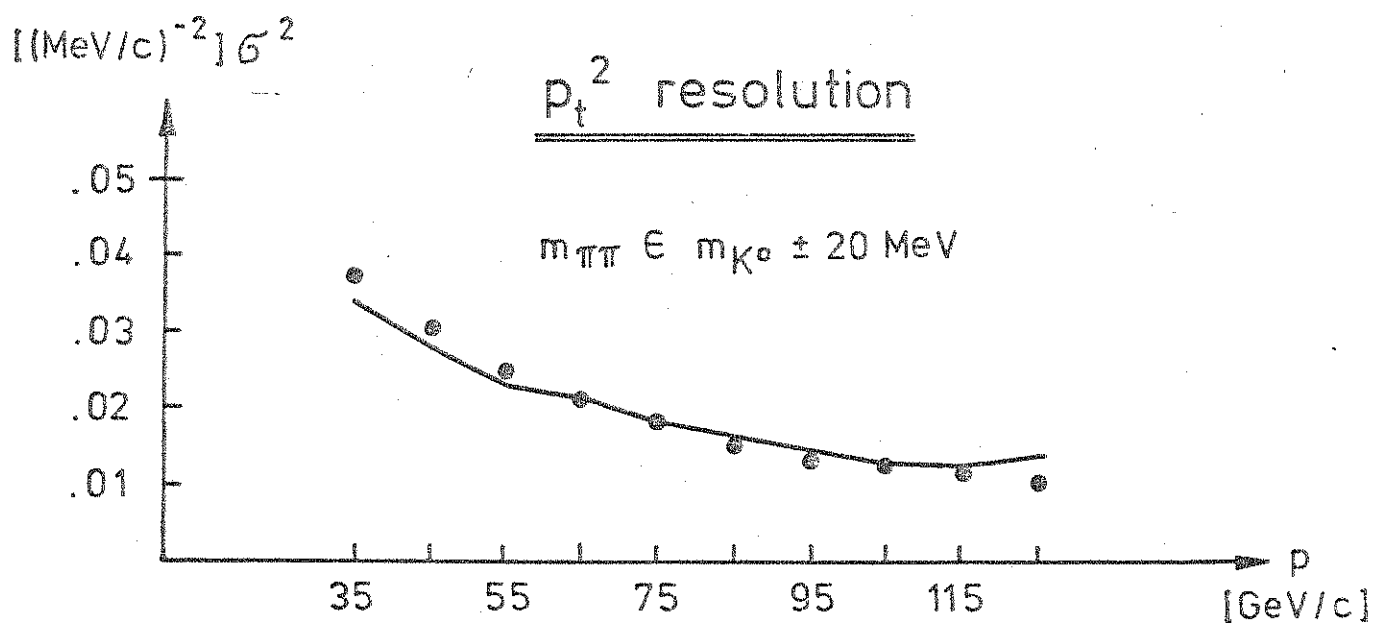
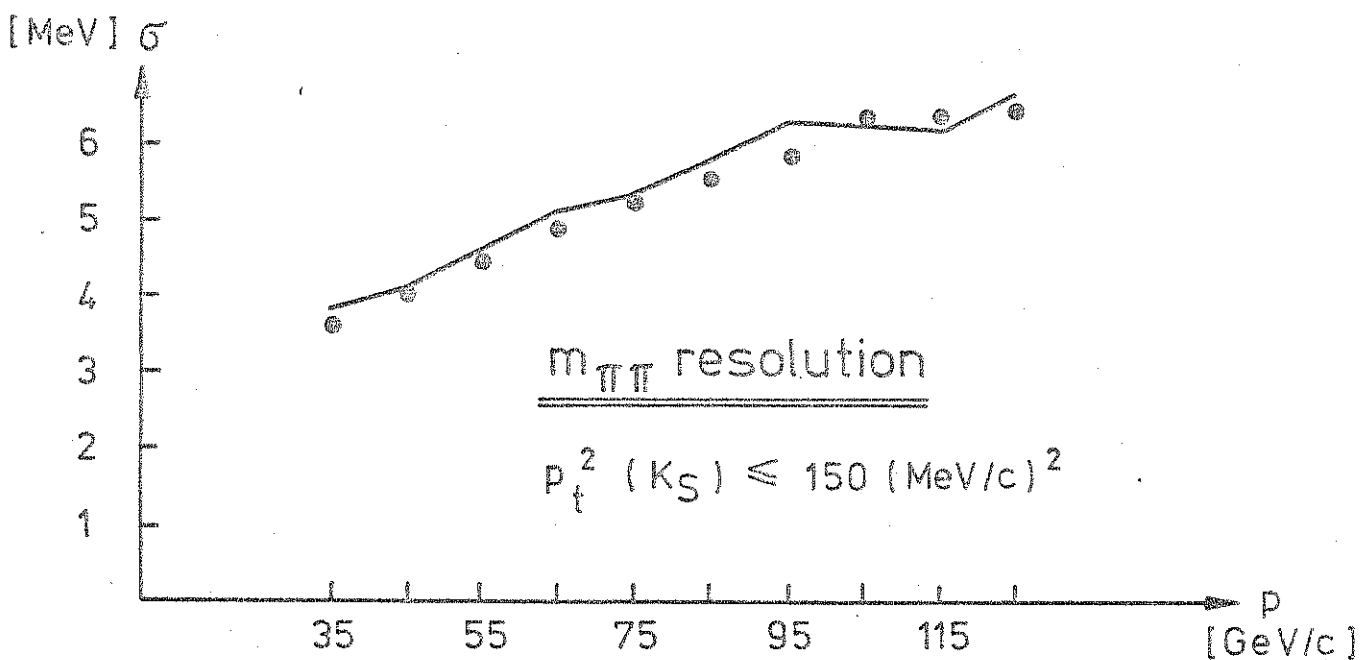


Fig. 5.6 $K\mu 3$ argument distribution. The vertical lines indicate the region of unambiguous momentum events used in the analysis. The K_L momenta for this distribution lie between 40 GeV/c and 60 GeV/c.

Data: —

M.C.: ●

$K\mu$ 3 Argument distribution.

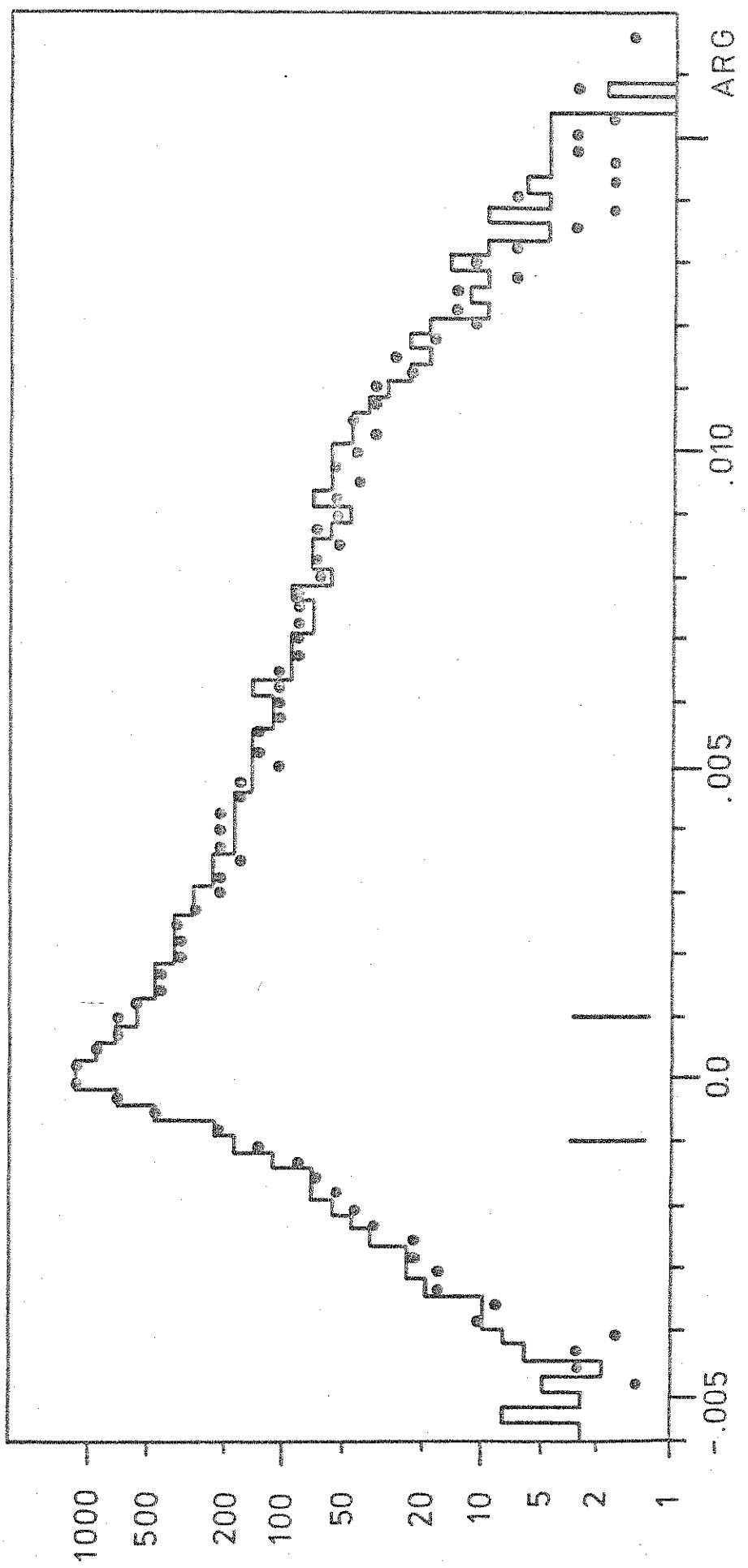


Fig. 5.7 $K\pi^2$ acceptance (integrated over the decay region) as a function of the kaon momentum.

Fig. 5.8 $K\mu^3$ acceptance (integrated over the decay region) as a function of the kaon momentum.

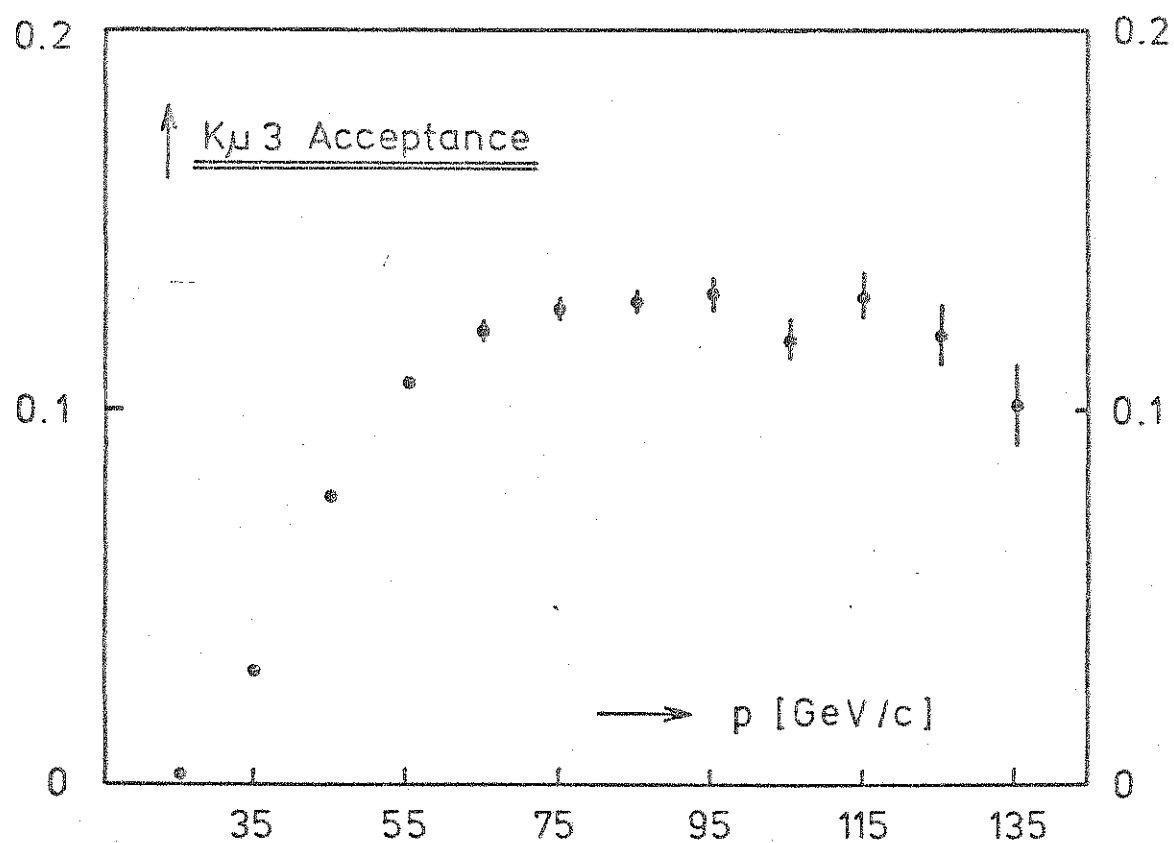
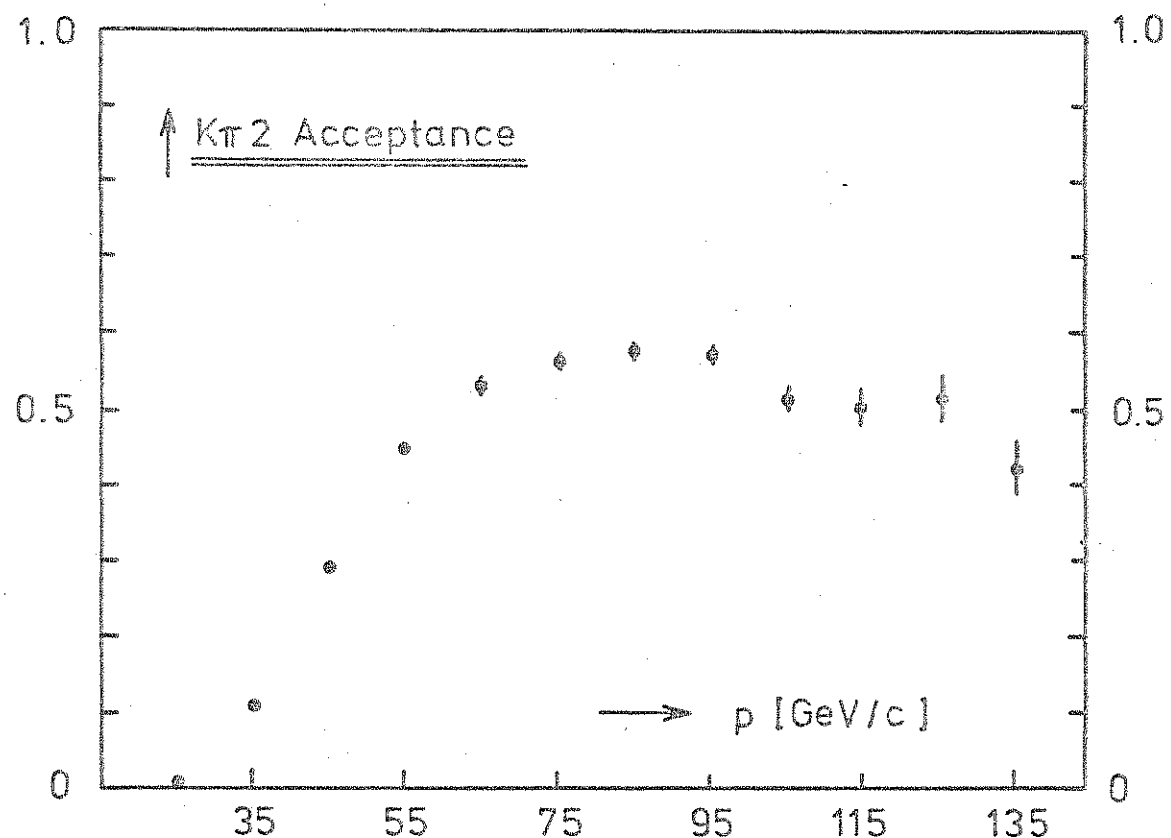


Fig. 6.1 Number of MWPC hits per event.

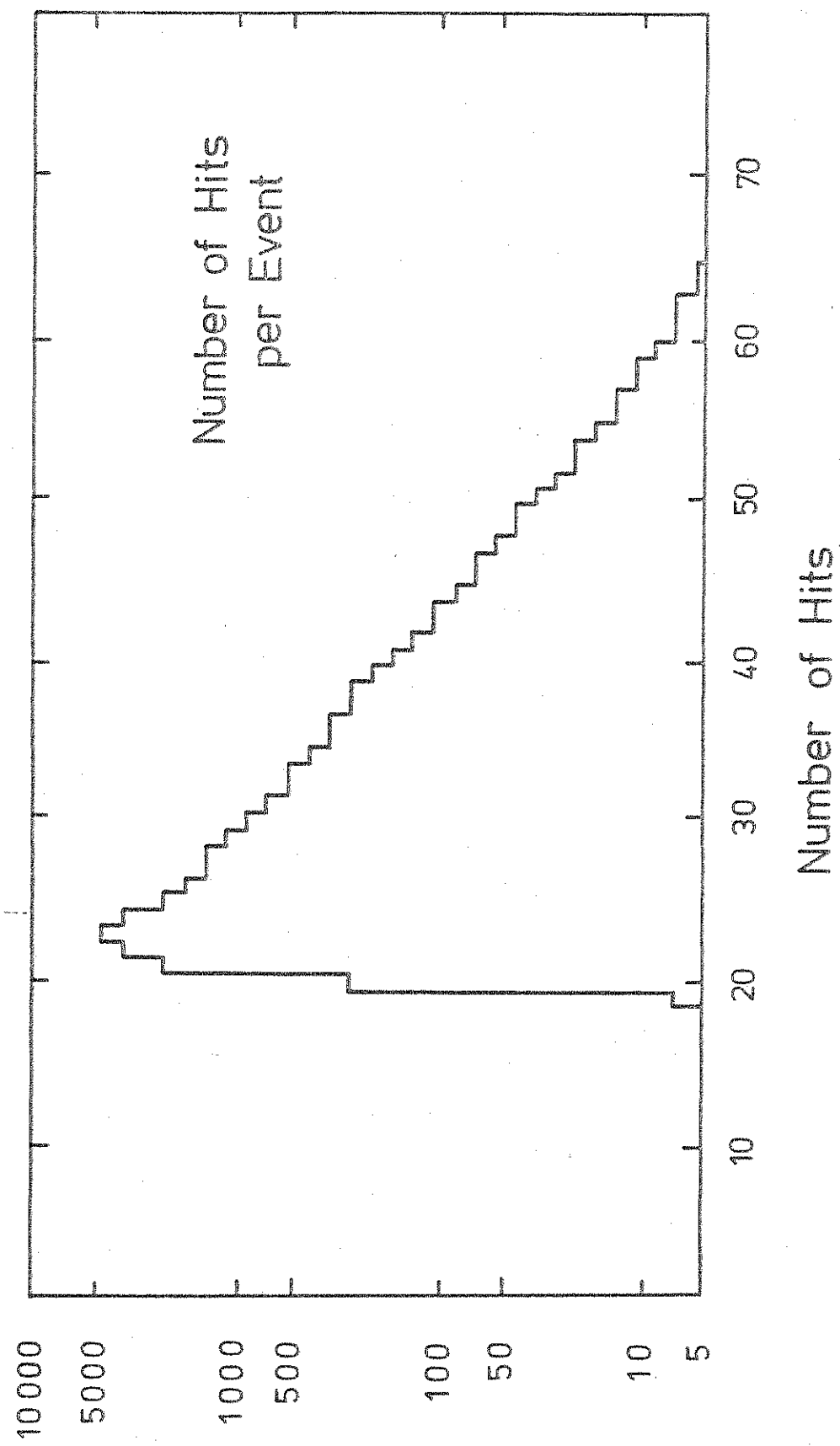


Fig. 6.2 Vertical profile of the reconstructed vertex position showing the two beams.

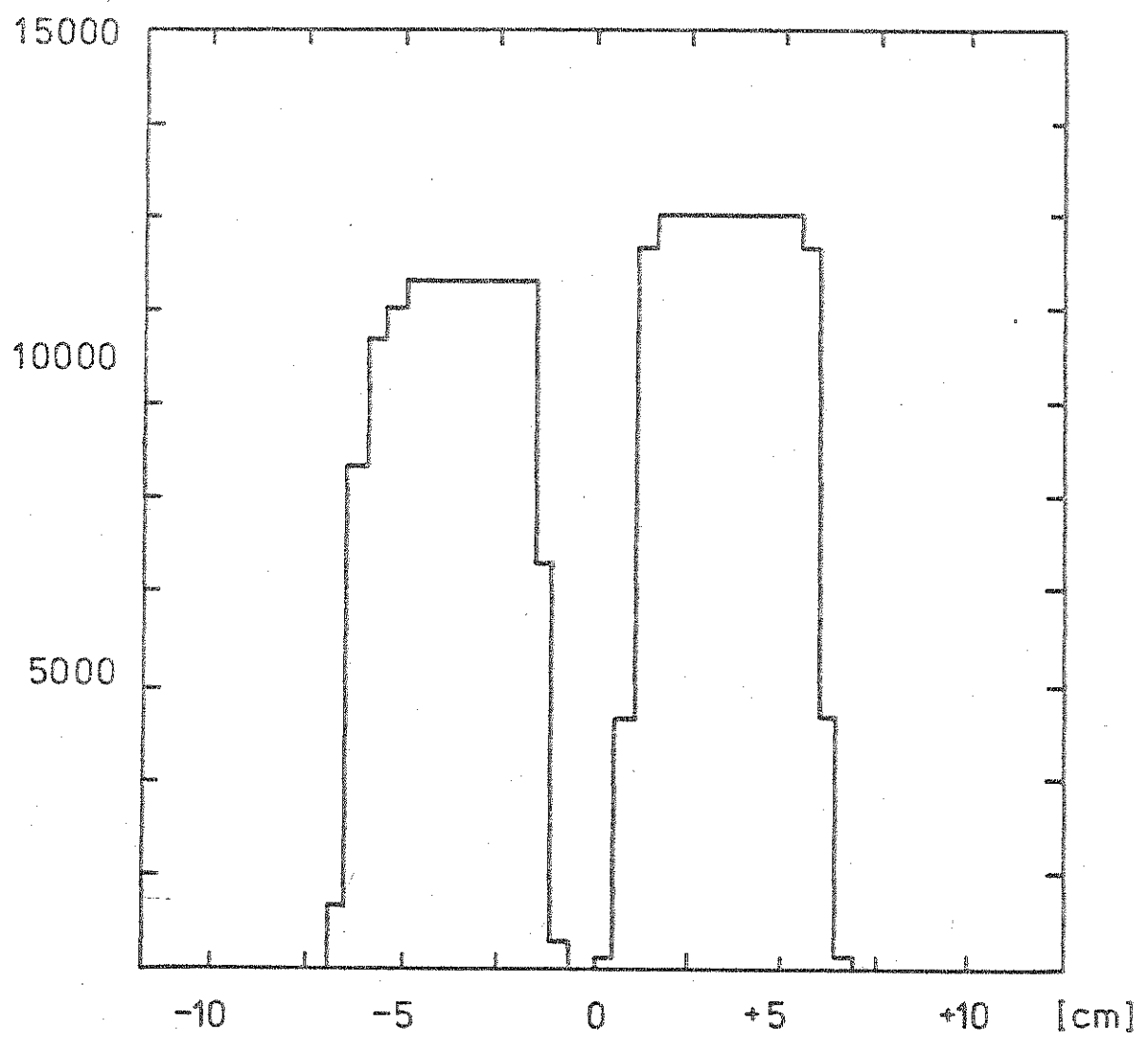


Fig. 6.3 Ratio of the higher beam attenuation over the lower beam attenuation versus the primary beam intensity. The scatter plot shows a clear correlation with the beam intensity.

Fig. 6.4 Beam attenuation calculated by combining the information from the two beams. The scatter plot shows this attenuation normalized by $\exp(-X/L)$ versus the primary beam intensity. No rate dependence effect is visible.

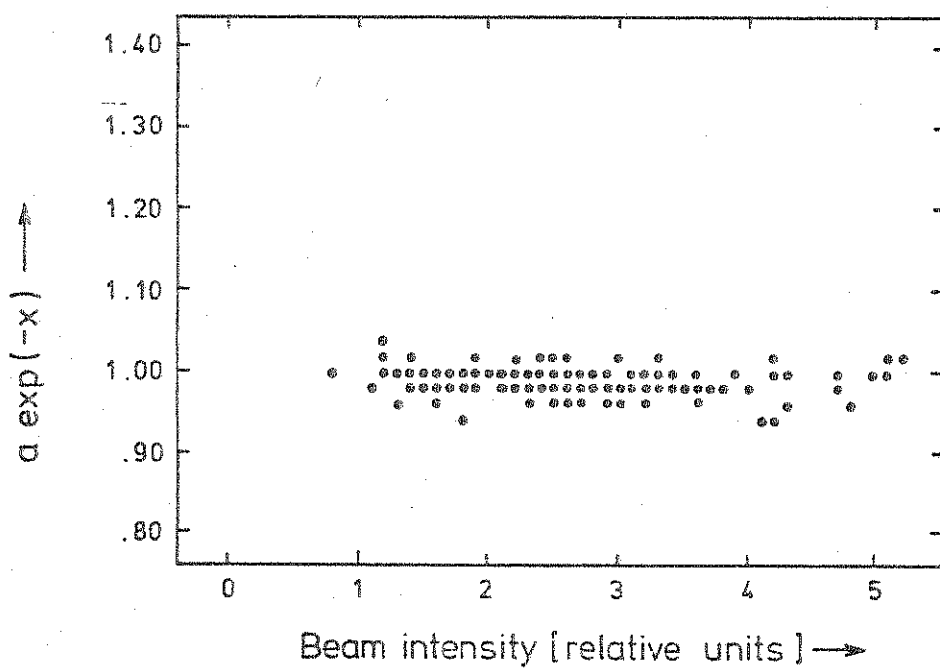
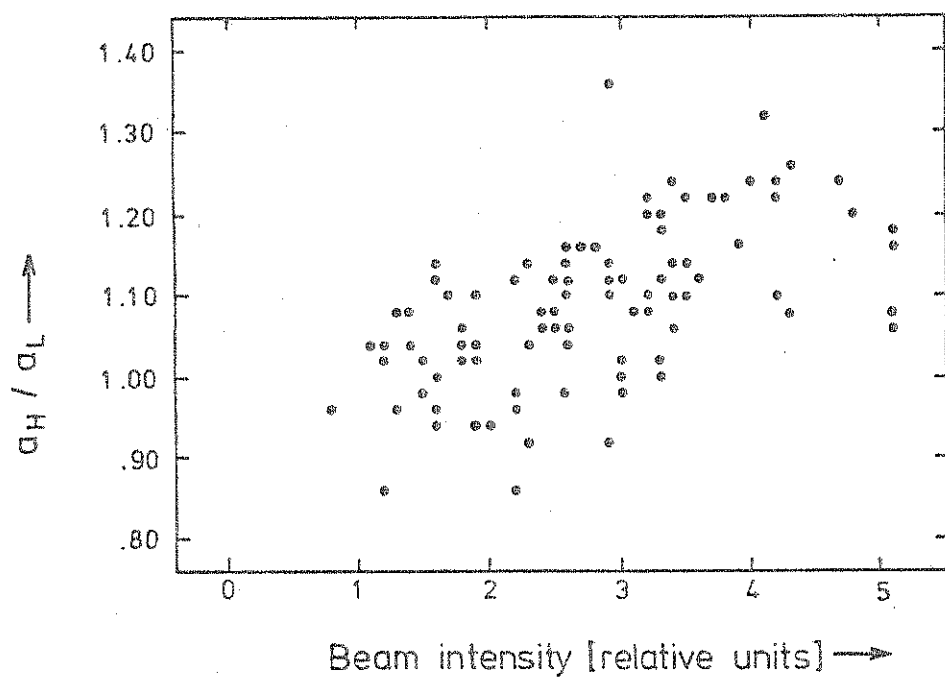


Fig. 6.5 Monte Carlo calculated probability of a kaon to scatter from one beam into the other (cross-talk) .

Fig. 6.6 Measured fraction of kaons detected in the plugged beam (plugged by filling one of the holes of the fixed collimator) as a function of the lead radiator thickness.

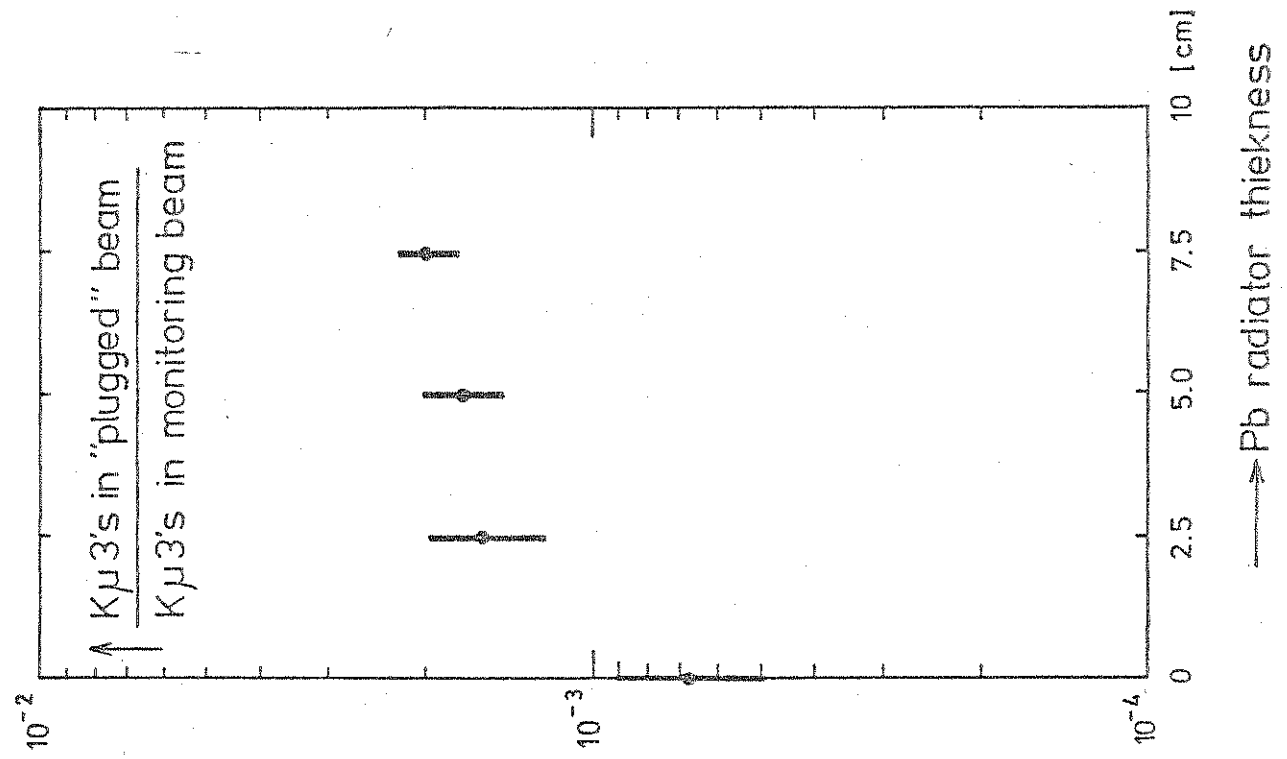
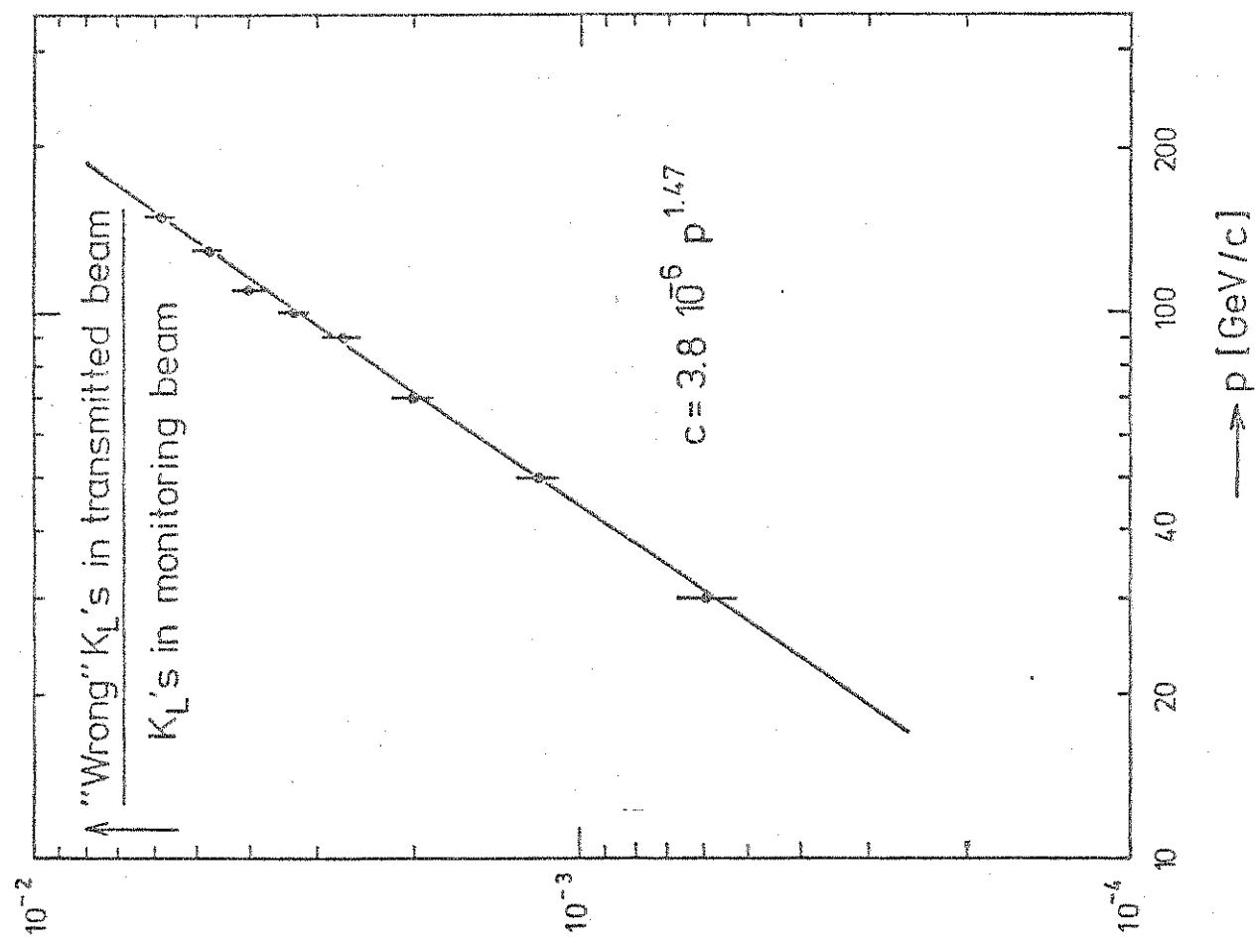


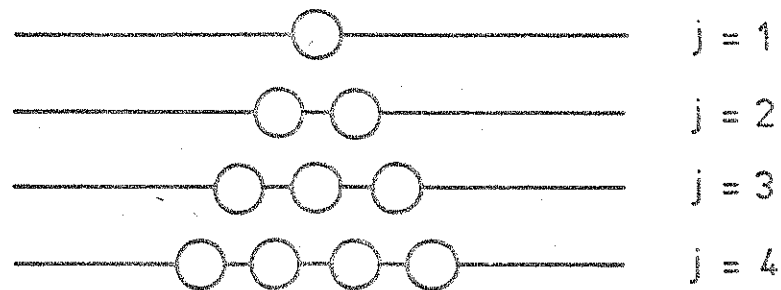
Fig. 7.1.a Typical elastic multiple-scattering diagrams included in the standard Glauber model.

Fig. 7.1.b Typical inelastic multiple-scattering diagrams included in the Karmanov-Kondratyuk model. The fat lines correspond to the propagation of the inelastic intermediate states.

Fig. 7.1.c Typical inelastic multiple-scattering diagrams not included in the Karmanov-Kondratyuk model, i.e.

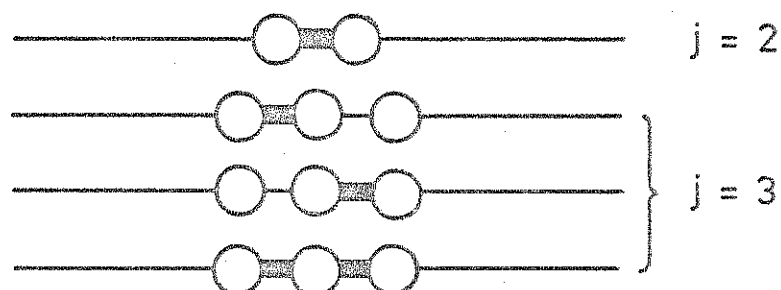
- multiple excitation/desexcitation of the projectile.
- double excitation of the projectile.

a)



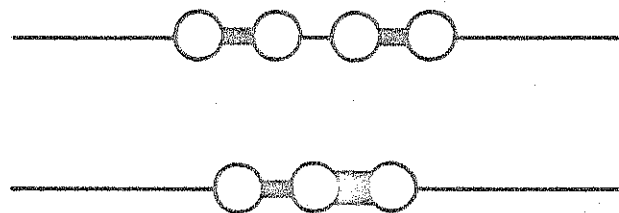
etc.

b)



etc.

c)



etc.

Fig. 8.1 Final results for the K_L total cross-sections.

The straight lines are best fits to our data.

• Present experiment (Unambiguous $K\mu 3^{\prime}$'s) .

△ Ref.⁴⁷

□ Ref.⁴⁸

○ Ref.⁴⁹

✗ Ref.⁵

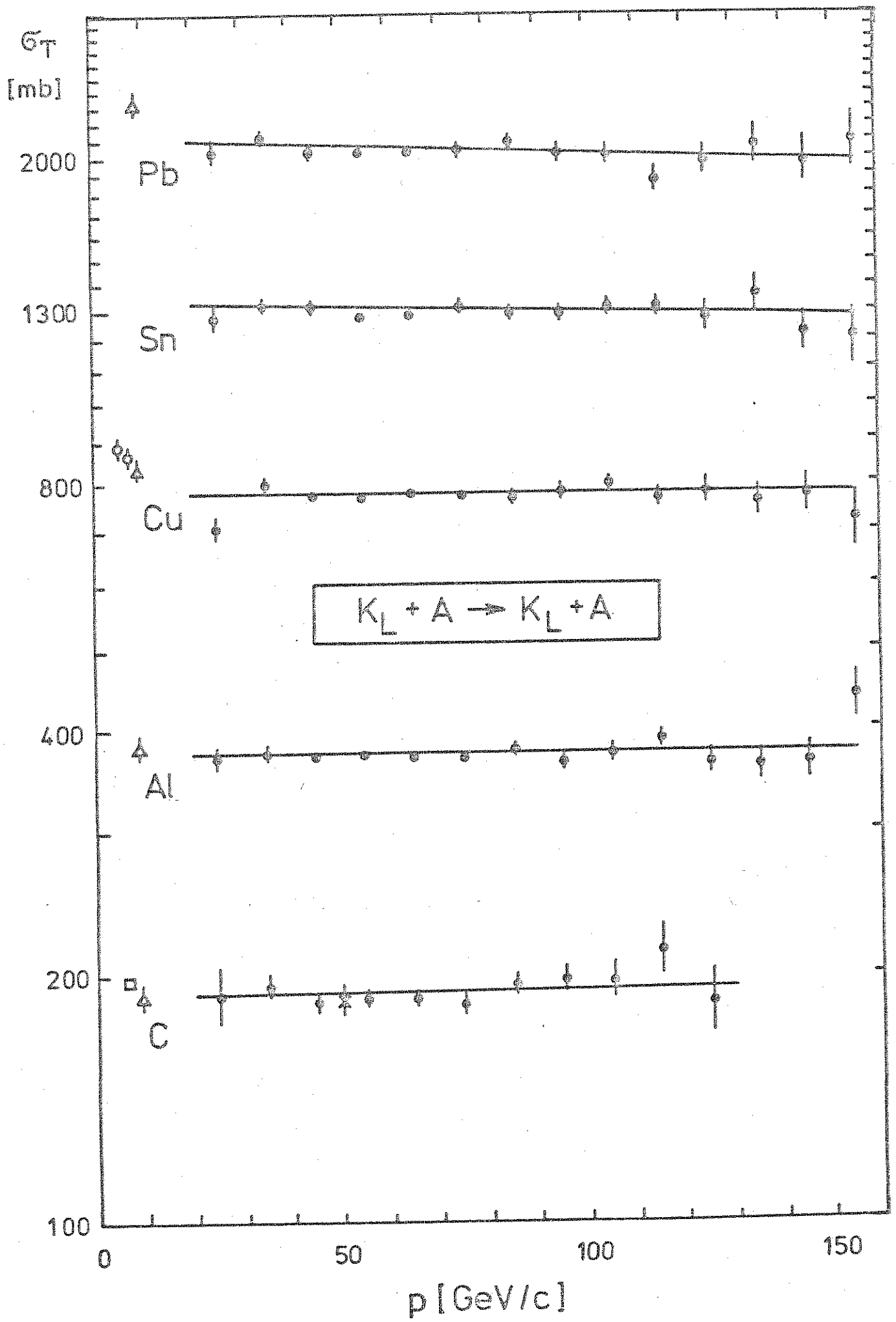


Fig. 8.2 Final results for K_S coherent regeneration. The lines are the best fits to $p^{\alpha-1}$ in the 25-135 GeV/c momentum range.

X Ref.³⁴ (Pb)

- This experiment for Al, Cu, Sn and Pb above 10 GeV/c.
- Ref.⁴⁶ (Pb)
- Ref.⁴⁹, Ref.⁵⁰ (Cu)
- Ref.⁵¹, Ref.⁵ (C)

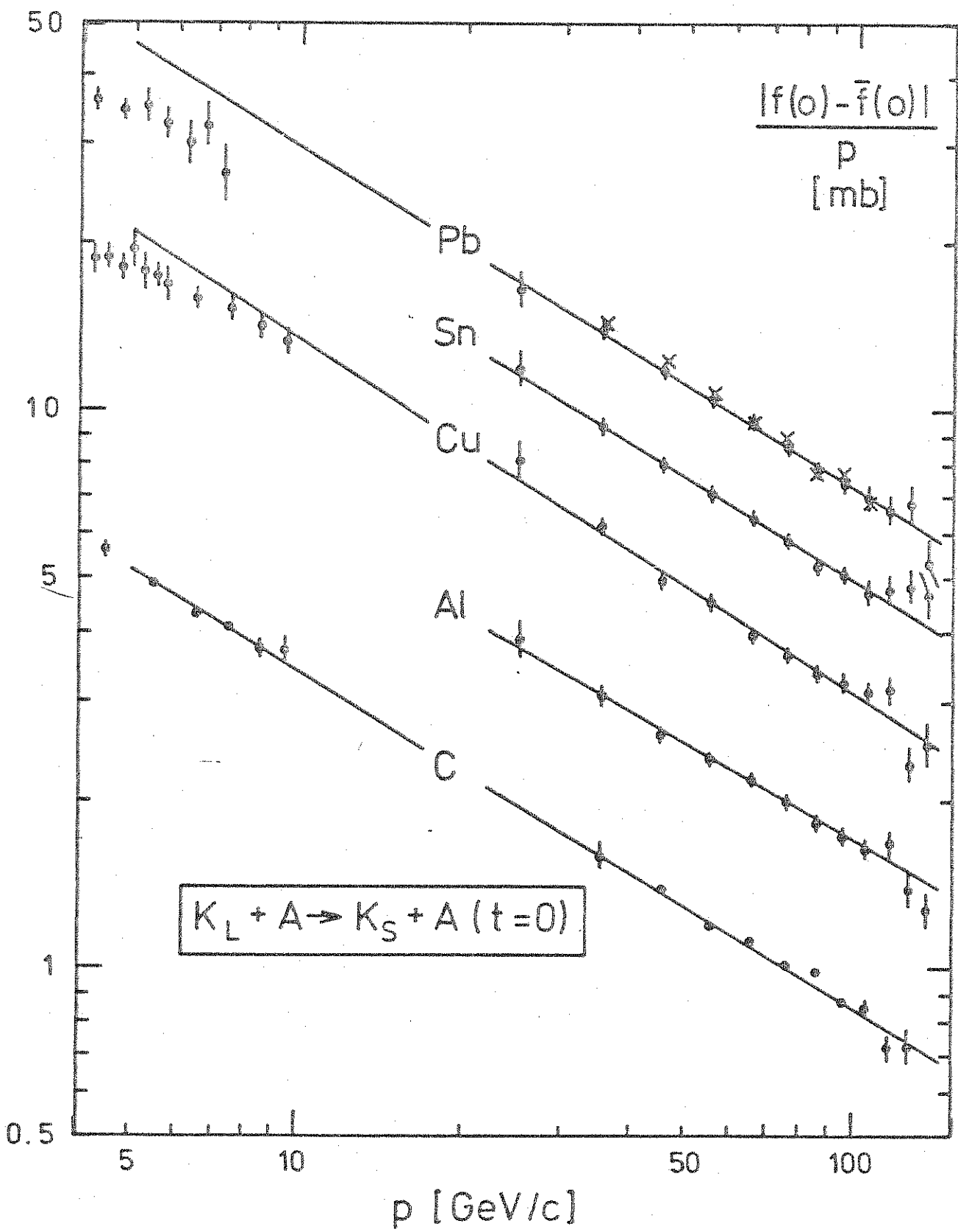
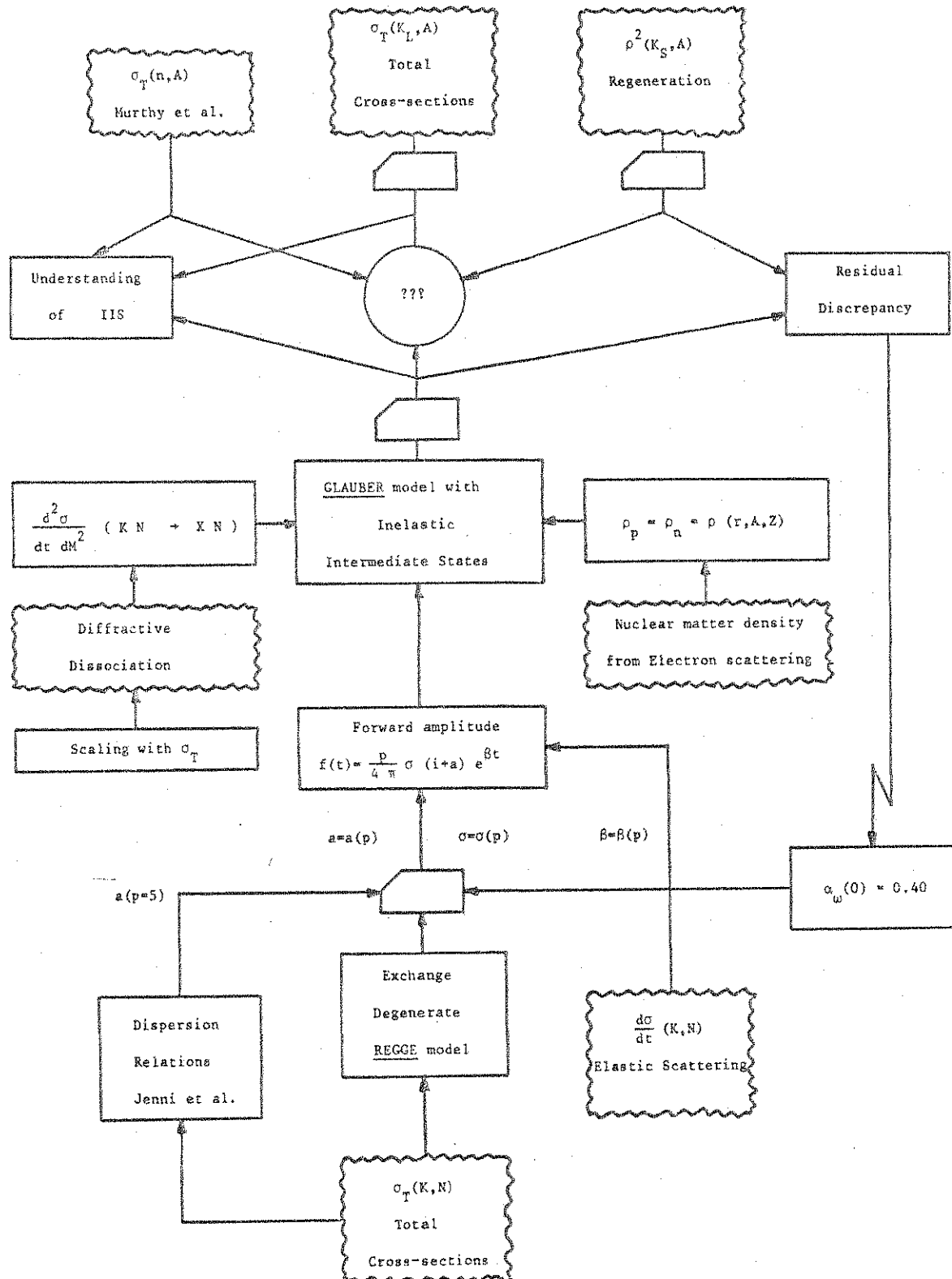


Fig. 8.3 Analysis organigram.



ANALYSIS ORGANIGRAM

Fig. 8.4 Comparison of model prediction of neutron-nucleus total cross-sections with the data. The data compilation is from Ref.⁴¹.
--- Glauber model without IIS.
— Glauber model with IIS.

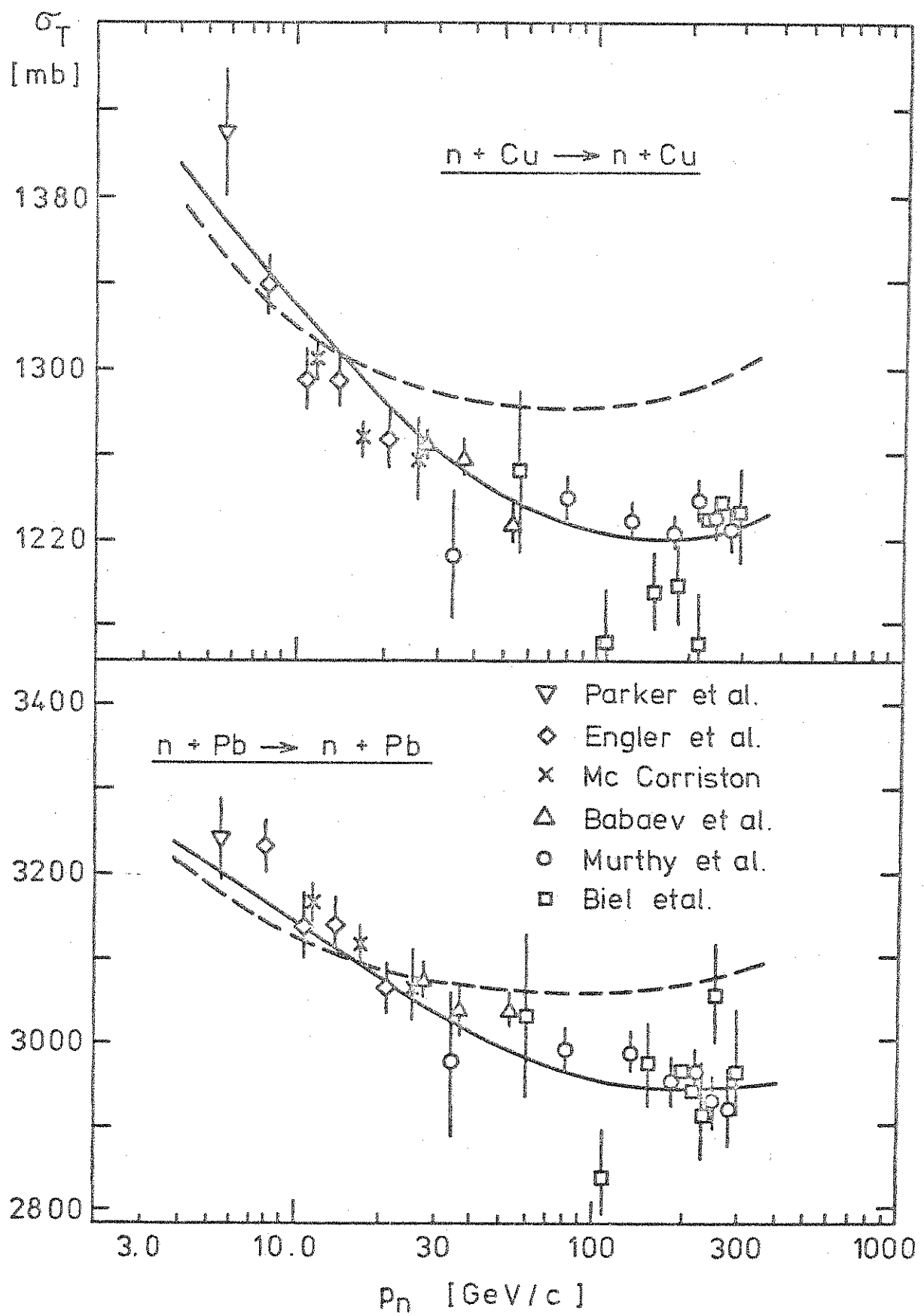


Fig. 8.5 "Measured" inelastic screening defect of neutron-nucleus total cross-section at 200 GeV/c as a function of atomic weight.

The solid line is our prediction (7.10). The data are from Ref.².

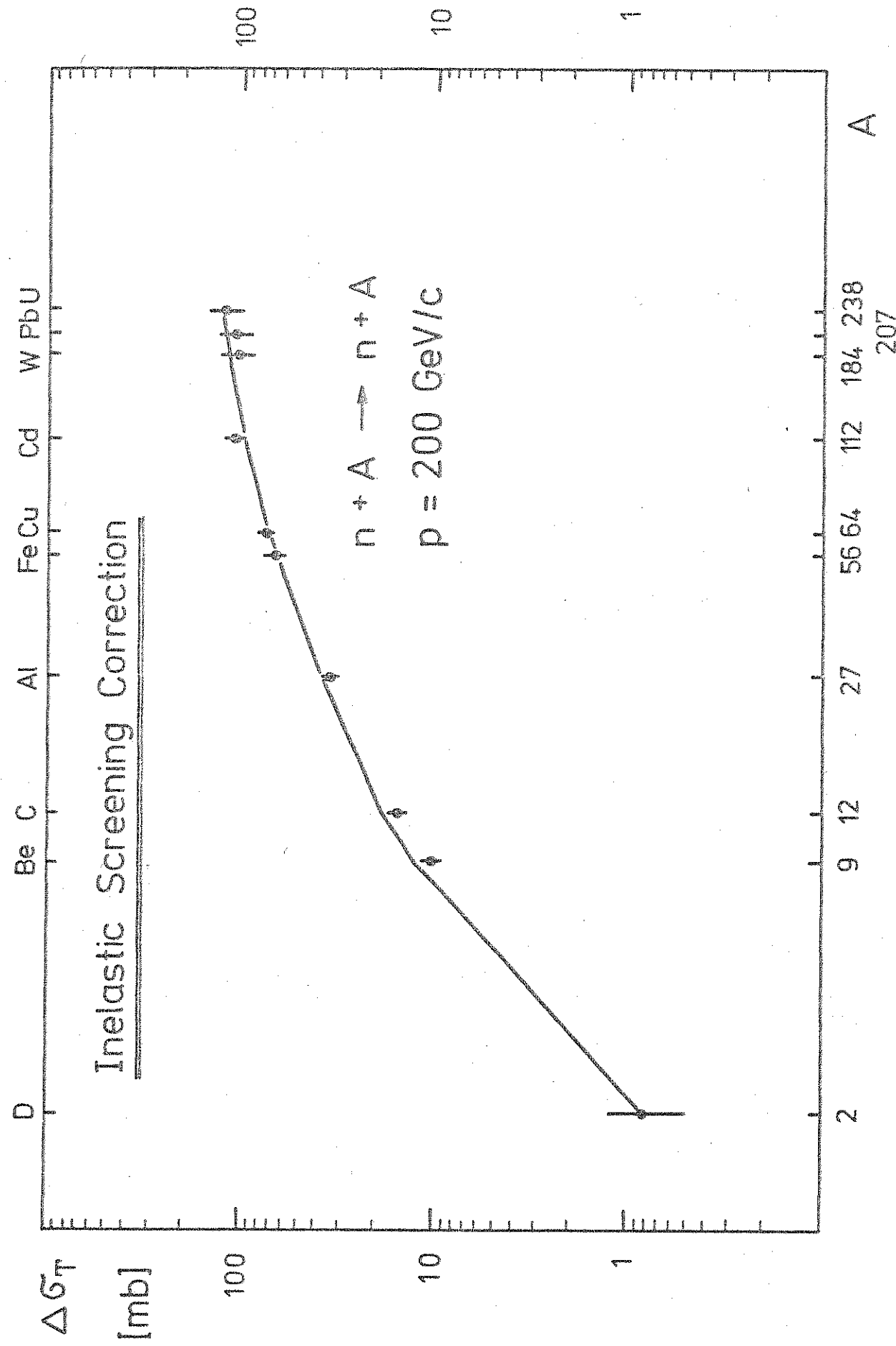


Fig. 8.6 Comparison of model predictions of kaon-nucleus total cross-sections with the data. The data are as in Fig. 8.1.

--- Glauber model without IIS.
— Glauber model with IIS.

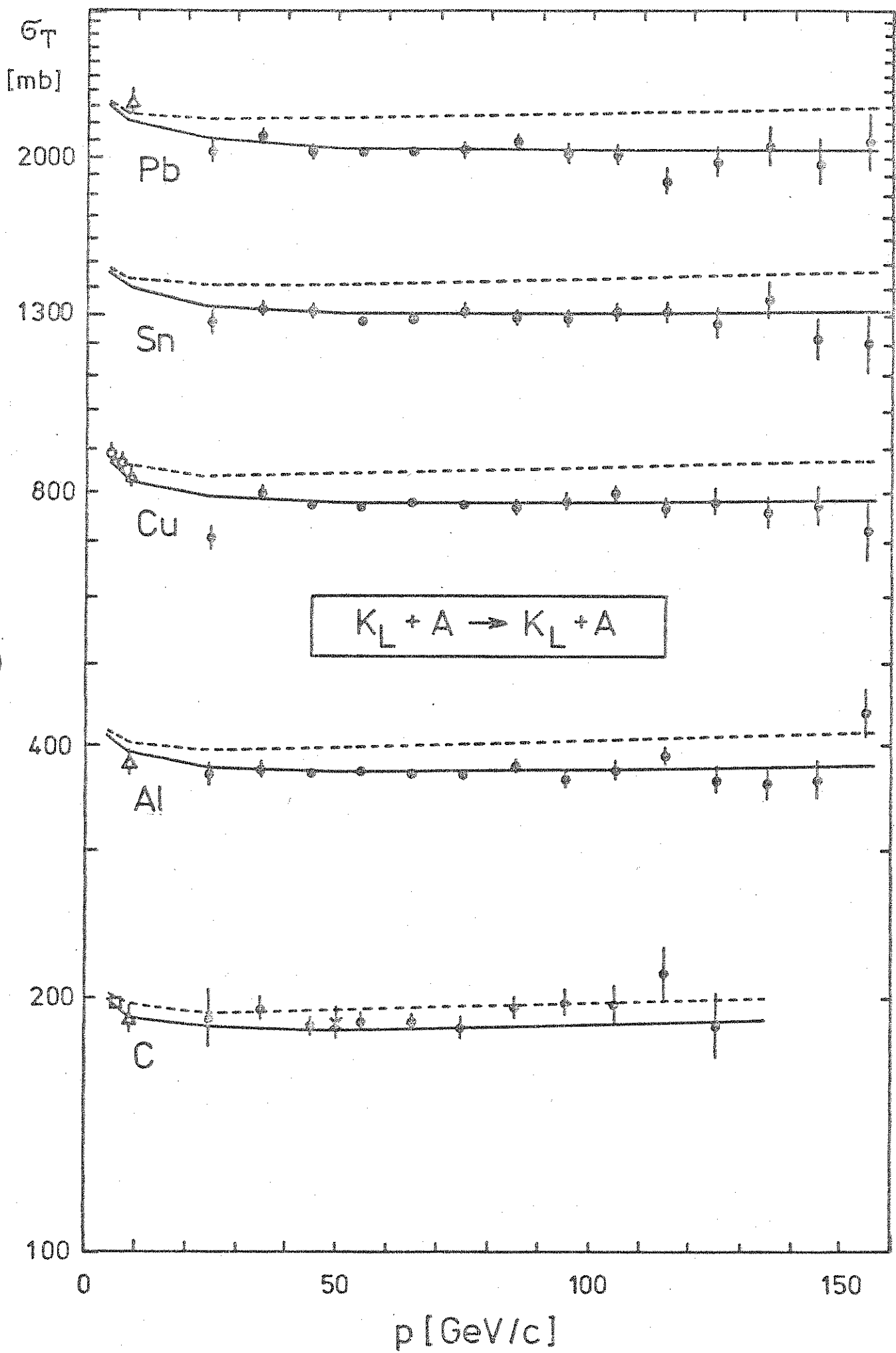


Fig. 8.7 "Measured" inelastic screening defect of kaon-nucleus total cross-section at 50 GeV/c as a function of atomic weight.
The solid line is our prediction (7.10).

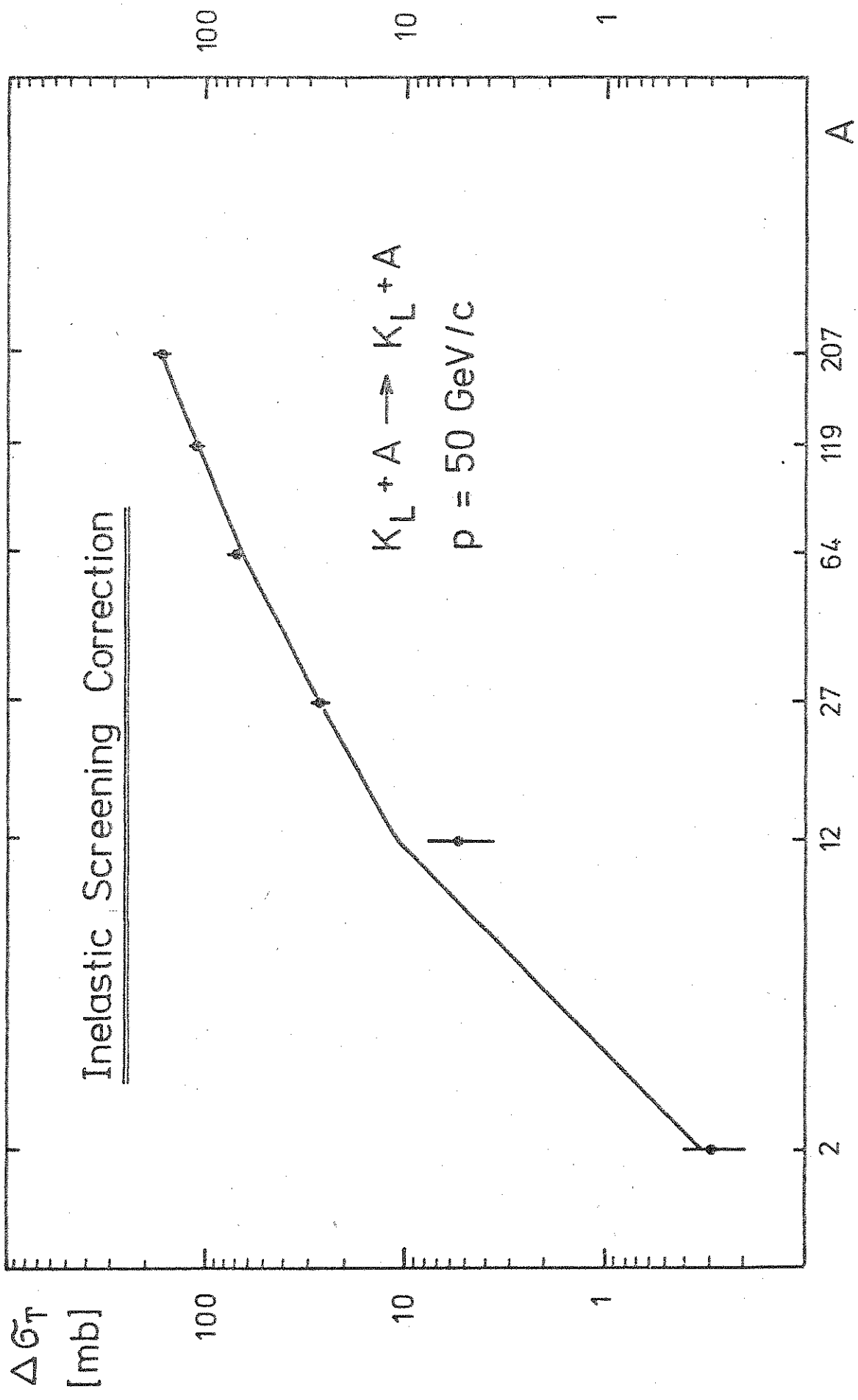


Fig. 8.8 Comparison of the inelastic screening correction at 50 GeV/c for kaons and neutrons as a function of atomic weight. In heavy nuclei the inelastic screening correction is much larger for kaons than for neutrons.

Relative inelastic screening Correction

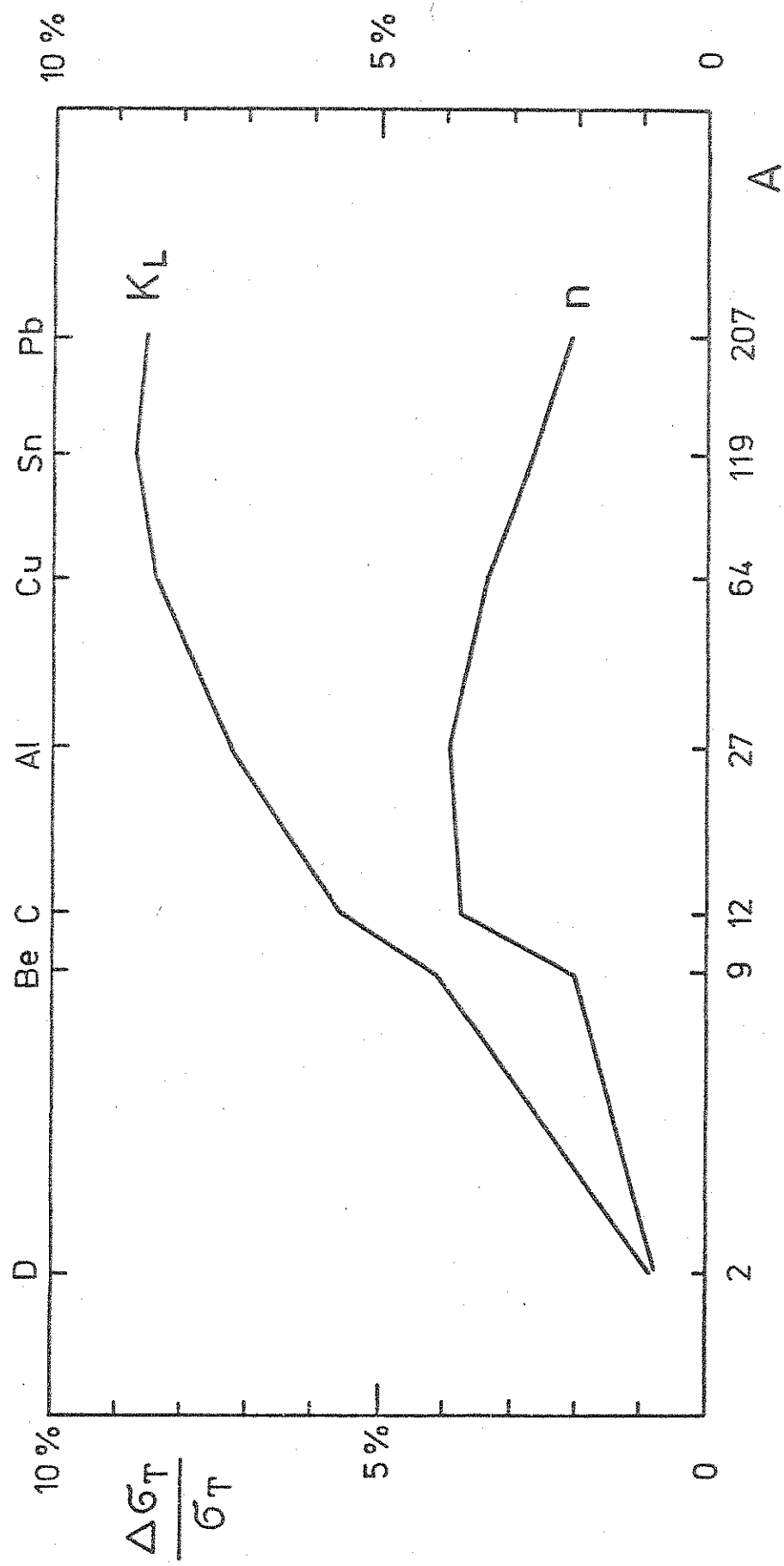


Fig. 8.9 Comparison of model predictions of K_S coherent regeneration with the data. The input elementary kaon-nucleon amplitudes are taken from standard Regge fits and dispersion relation calculations. The Glauber model, even with the contribution of inelastic intermediate states, disagrees with the data. The data is as in Fig. 8.2 .

---Glauber model without IIS.

—Glauber model with IIS.

N.B.: The Glauber model input amplitudes parametrization is given in Table 8.8, fit (i) .

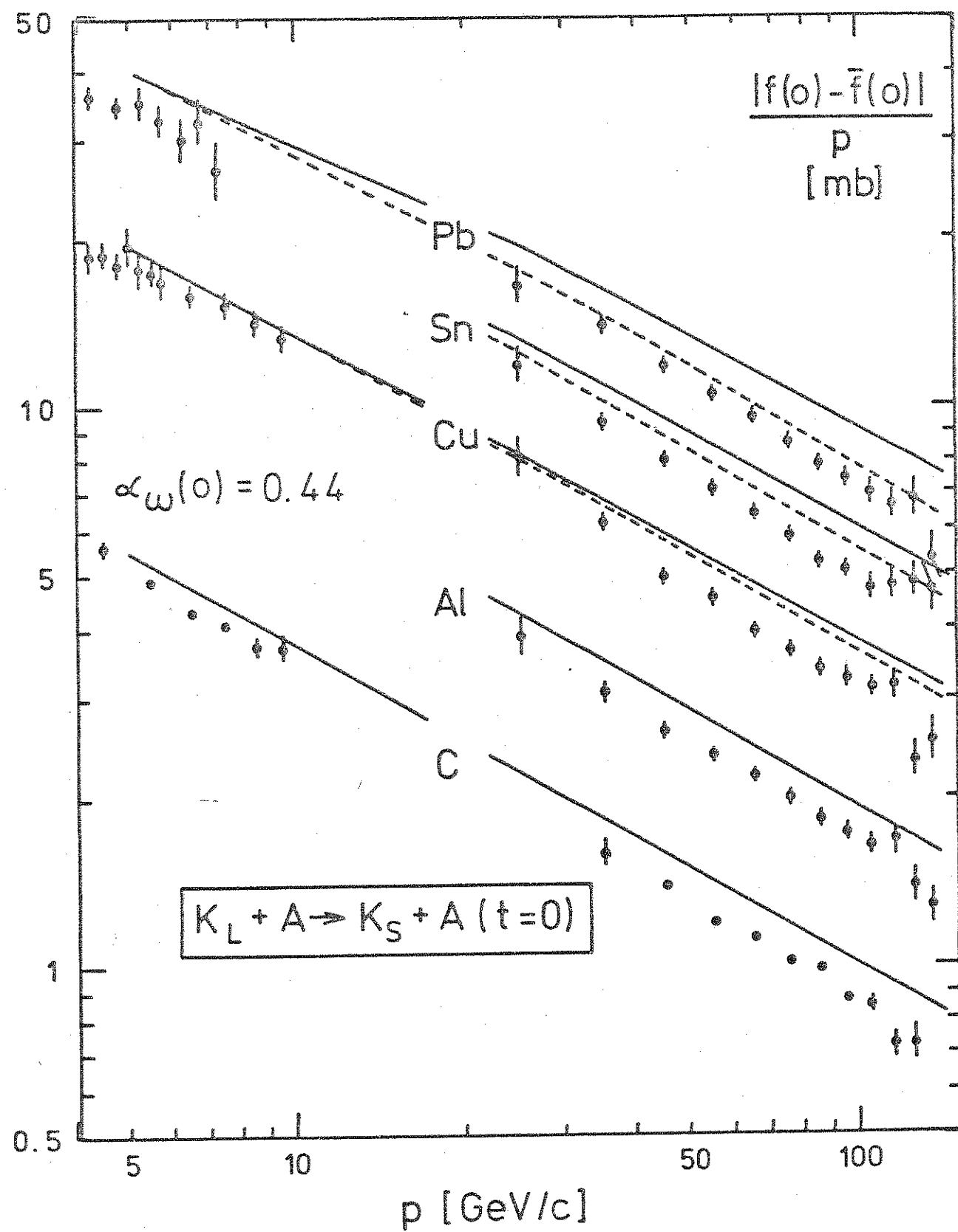


Fig. 8.10 Comparison of model predictions of coherent K_S regeneration with the data. The input elementary kaon-nucleon amplitudes are constrained to fit the carbon power law momentum dependence. The Glauber model with inelastic intermediate states is now in good agreement with the data. The data is the same as in Fig. 8.2 .

--- Glauber model without IIS.

— Glauber model with IIS.

N.B.: The Glauber model input amplitudes parametrization is given in Table 8.8, fit (iii) .

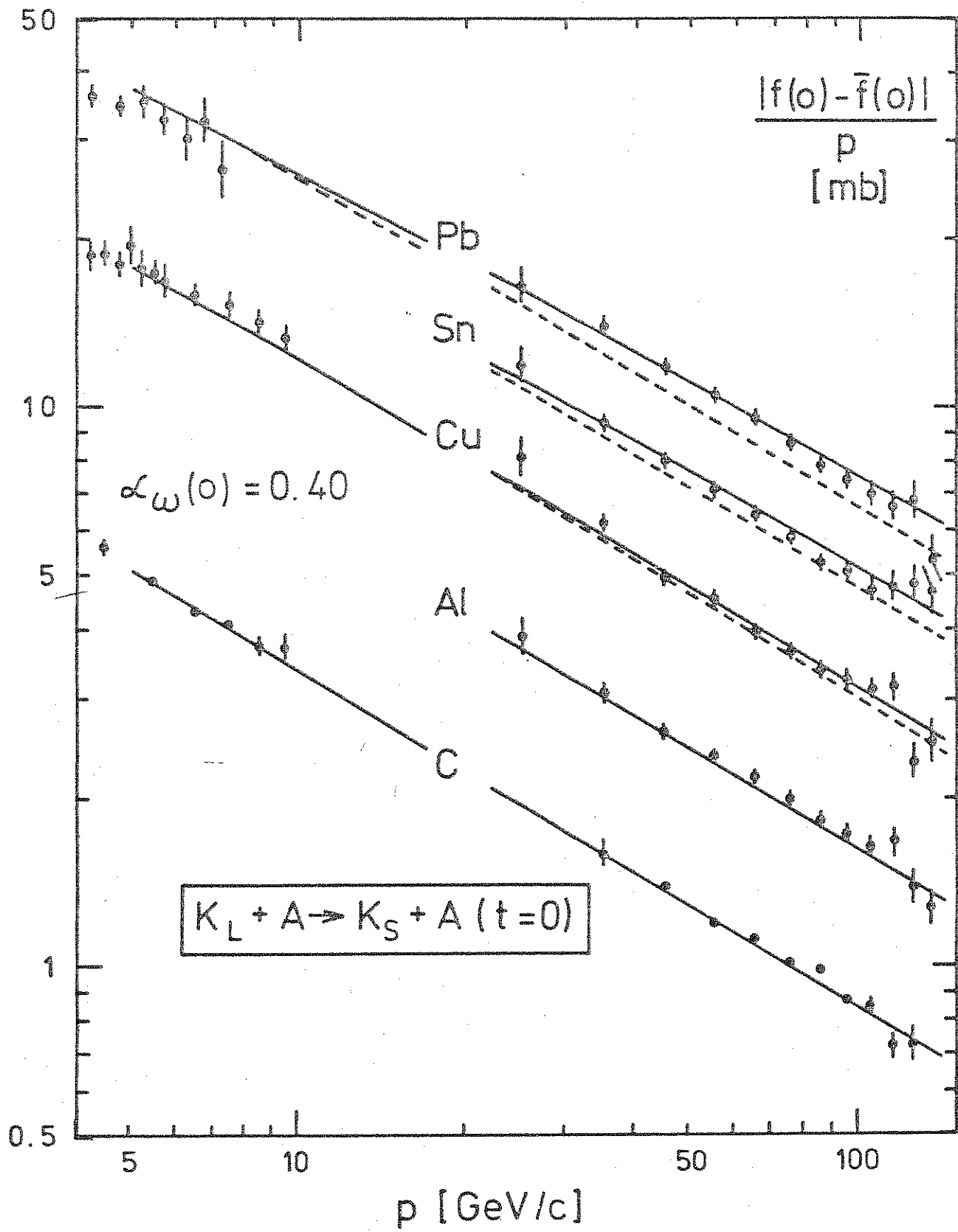


Fig. B.1 Comparison of Regge model predictions of charge exchange reactions with the data. The data are from Ref.³¹.

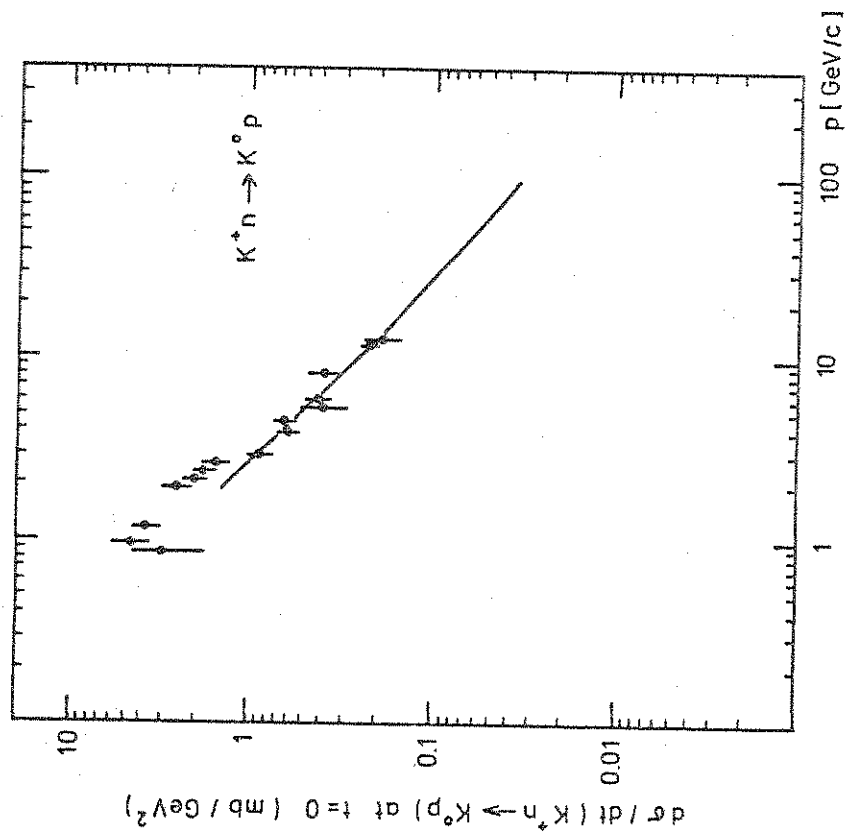
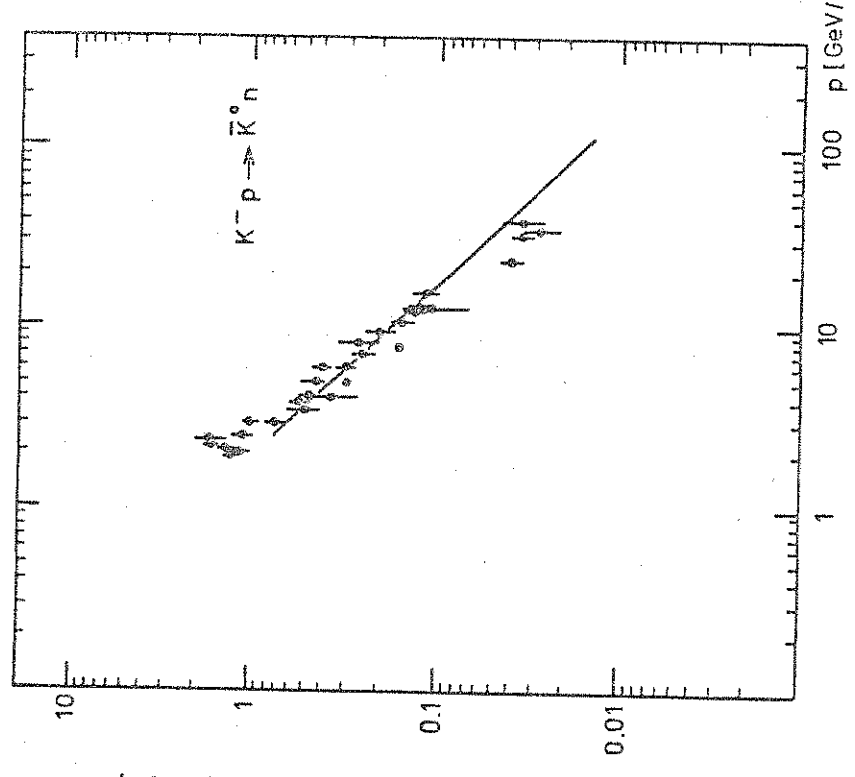


Fig. B.2 Comparison of Regge model predictions of K_S regeneration on proton with the data. The normal Regge prediction with $\alpha_{\omega}(0)=0.44$ agrees with the data, but the prediction constrained with $\alpha_{\omega}(0)=0.40$ (as required by K_S regeneration on carbon) disagrees with the data.

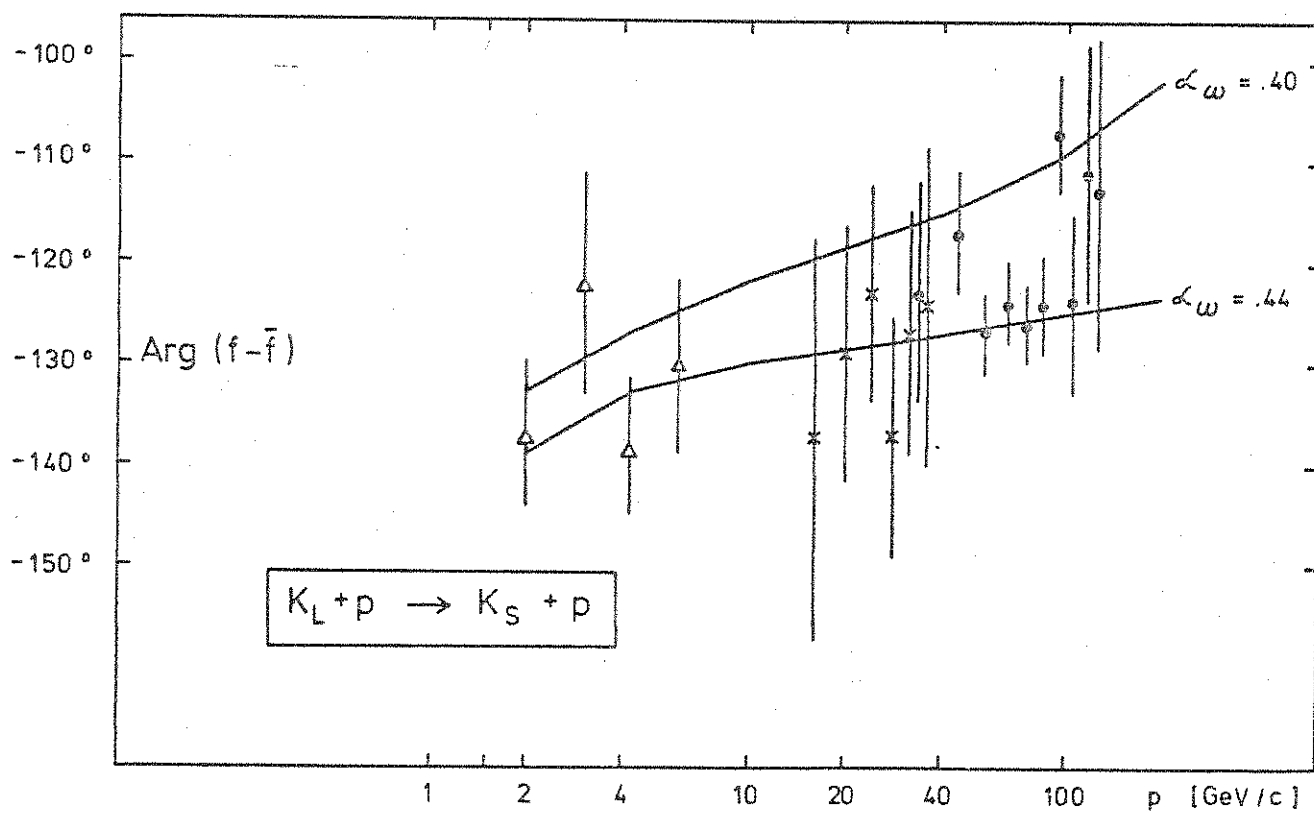
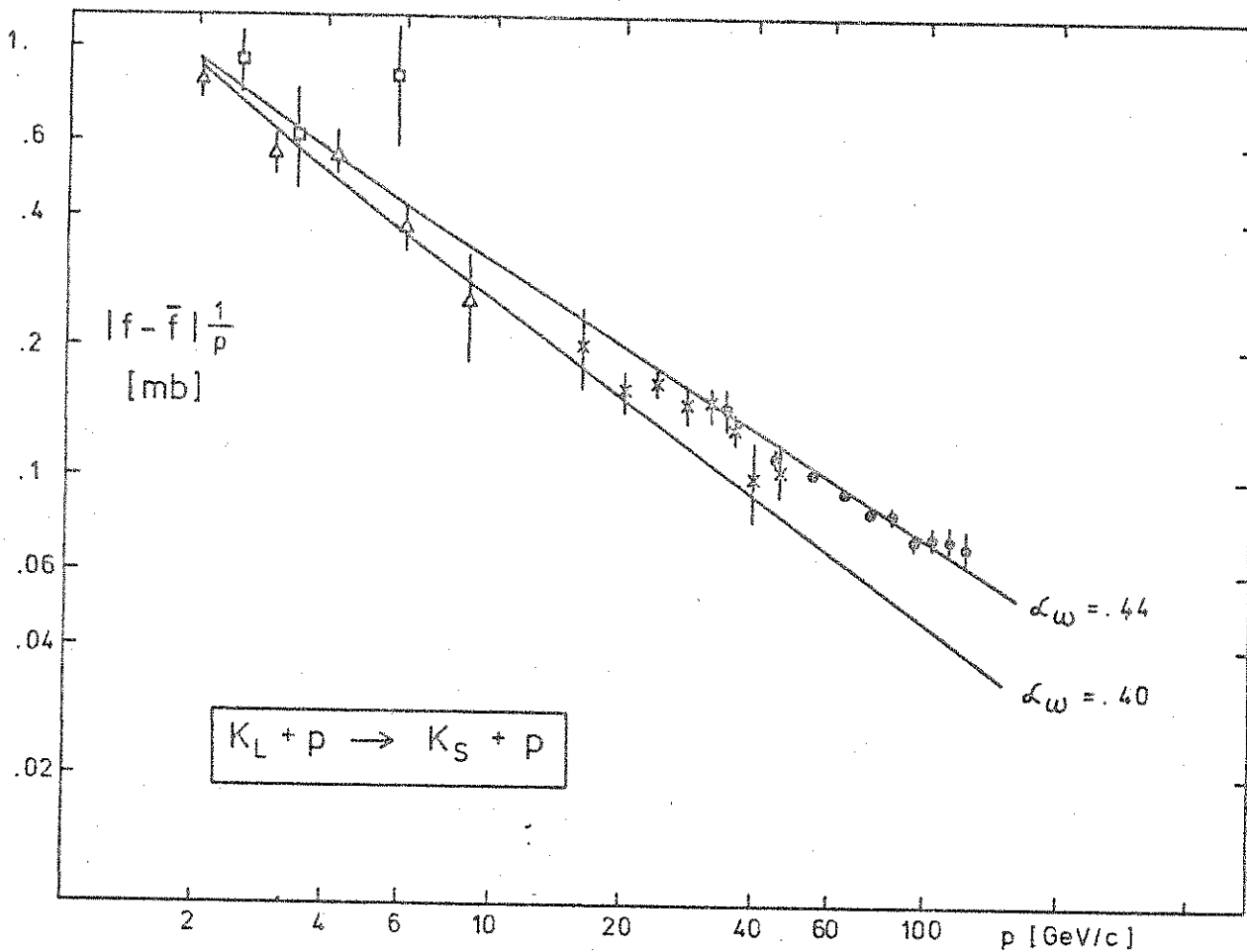
◻ Ref.⁵²

△ Ref.⁵³

✗ Ref.⁵⁴

● Ref.¹⁴

N.B.: The Regge fits used for these two predictions are respectively fit (i) and fit (iii) of Table 8.2 .



CURRICULUM VITAE

I was born on the 29th of March 1948 in Brig (VS) . In 1958 I moved with my family to Lausanne. I attended the secondary school, and later the Gymnasium where I obtained the baccalaureat in 1967. I then immatriculated at the faculty of Sciences of the University of Lausanne, and graduated in physics in 1972. Since then I have been working at CERN until 1975, and thereafter, under the sponsorship of Prof. V.L. Telegdi, at Fermilab near Chicago until 1977. Currently I am working at CERN in the ETH-Ecole Polytechnique-Strasbourg collaboration.